Reactive and Functional Polymers xxx (2016) xxx–xxx

Contents lists available at ScienceDirect

Reactive and Functional Polymers

journal homepage: www.elsevier.com/locate/react

Review

Highly transparent polyimide hybrids for optoelectronic applications

Chia-Liang Tsai [a,1], Hung-Ju Yen [b,1], Guey-Sheng Liou [a,*]

[a] Functional Polymeric Materials Laboratory, Institute of Polymer Science and Engineering, National Taiwan University, 1 Roosevelt Road, 4th Sec., Taipei 10617, Taiwan
[b] Physical Chemistry and Applied Spectroscopy (C-PCS), Chemistry Division, Los Alamos National Laboratory, Los Alamos, NM 87545, USA

ARTICLE INFO

Article history:
Received 12 March 2016
Received in revised form 24 April 2016
Accepted 26 April 2016
Available online xxxx

Keywords:
Polyimide
Hybrid material
TiO_2
ZrO_2
silver nanowire

ABSTRACT

Polyimides comprising high polarized moieties and electron-withdrawing groups usually exhibit high refractive index and good transparency with great potential for optoelectronic devices. Particularly, the incorporation of hydroxyl groups on the backbones of polyimides is an important strategy to enhance the solubility and provide reactive sites for organic-inorganic bonding. Composites prepared from organic polymer binder and inorganic fillers have recently attracted considerable interests due to their enhanced mechanical, thermal, optical and electrical properties compared to the corresponding polymer or inorganic component. Moreover, the inorganic components in hybrid films can also serve as electron acceptors for stabilizing the charge transfer complex thus result in electrically programmable digital memory properties. In addition, the high performance polyimides can further served as substrate and protector for the AgNWs-polyimide conductive hybrid films, exhibiting good adhesive property, high bendability, and excellent thermal stability. Owing to the high glass transition temperature (T_g) of polyimides, the resulted AgNWs-polyimide electrode can maintain its conducting performance at high temperature operation. Thus, the hybrid electrode provided extremely high potential to operate at harsh working environment or further post processing. By the excellent combination of transparent polyimides and inorganic materials, the resulting polyimide hybrids showing promising potential are indispensable to optical and electrical applications.

Contents

* Corresponding author.
E-mail address: gsliou@ntu.edu.tw (G.-S. Liou).
[1] These authors contributed equally to this work.

http://dx.doi.org/10.1016/j.reactfunctpolym.2016.04.021
1381-5148/

1. Introduction

1.1. High performance polymers

Materials science is an interdisciplinary and fundamental field of engineering that focuses on designing the most suitable materials for appropriate applications. Ceramics, metals, and polymers are three main categories of materials till now. Among of these materials, polymer is the most common material that is always applied in daily essentials, such as desks, chairs, packages, containers, clothes and so on. However, polymer science was unobtrusive and developed relatively late until Hermann Staudinger proposed a landmark paper in 1920 that rubber and other natural substances such as starch, cellulose, and proteins are long chains of short repeating molecular units linked by covalent bonds [1], which won him the 1953 Nobel Prize in Chemistry. In next two decades, polyamide (nylon), polyethylene (PE), polytetrafluoroethylene (Teflon) and silicon epoxy resin (silicone) had been successfully synthesized and largely utilized in several applications due to the advantages of low cost and lightweight. Furthermore, high-performance polymers were then developed in late 1950s in order to satisfy the demands on military, aerospace, buildings, and industrial applications. Owing to the great combination of extraordinary chemical, physical and thermomechanical properties, high performance-polymers have drawn many scientists' attention that make all-out effort on macromolecular design and polymer chemistry.

High-performance polymers were even developed much rapider in next decade of 1960. During that time, the introduction of aromatic segments into polymers was first pointed out by Hill and Walker [2] and mainly focused on enhancing their thermal stability. According to the theory mentioned above, many scientists selected aromatic units or heterocyclic rings to prepare functional high-performance polymers. Therefore, several commercialized high-performance polymers have been developed, such as Kapton®, Kevlar®, Lexan®, and other heterocyclic polymers (Scheme 1.1), which also demonstrate the useful information and importance for the molecularly structural design of new high-performance polymers.

1.1.1. Preparation of aromatic polyimides (PIs)

Among the polymeric materials, aromatic polyimides (PIs) have been recognized as one of the important high-performance polymers for industrial applications such as electronic packaging or flexible substrates due to the outstanding thermal stability and mechanical properties. In 1956, Endrey worked on his research assignment to find a solution processable method of aromatic PIs. Thus, he evaluated several organic solvents such as *N*,*N*-dimethylformamide (DMF) for poly(amic acid) (PAA, precursor of PI) and synthesized the first PAA film based on oxydianiline-pyromellitic dianhydride (ODA-PMDA). Next ten years, the production line of aromatic PI named as Kapton was set up successfully [3]. Kapton is a useful material that served as insulated layer of transformer and capacitor. In addition, other outstanding aromatic PIs have also been synthesized, such as Upilex, LARC-TPI, and Ultem. Therefore, the kingdom of high-performance PIs was built up step by step and used widely for many applications. The aromatic PIs were typically prepared by two synthetic routes: one-step and two-step polymerization methods which started from monomers of diamine

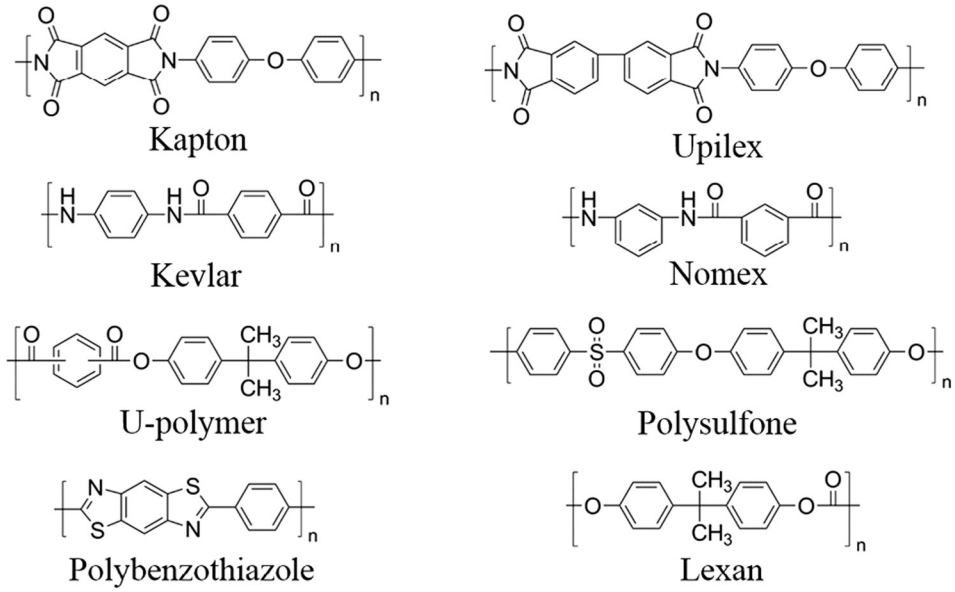

Scheme 1.1. Structures of several commercially available high-performance polymers.

Please cite this article as: C.-L. Tsai, et al., Highly transparent polyimide hybrids for optoelectronic applications, Reactive and Functional Polymers (2016), http://dx.doi.org/10.1016/j.reactfunctpolym.2016.04.021

and dianhydride.

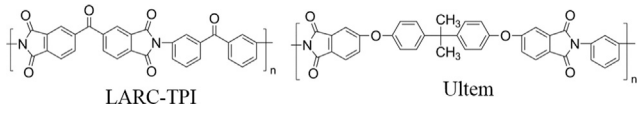

Two-step polymerization is the most widely utilized procedure to prepare aromatic PI. An aromatic tetracarboxylic dianhydride is added to a solution of aromatic diamine in a polar aprotic solvent such as *N,N*-dimethylacetamide (DMAc). After reacted for a while, the formed viscous PAA precursor are processed into shaped products, and then the cyclodehydration procedure is conducted by heating (thermal imidization) or treatment of chemical dehydrating agents (chemical imidization) [4].

The typical heating process is indicated as following: heating the PAA precursor from room temperature to 100 °C, 200 °C, then 300 °C, and hold for an hour for each step [5]. However, it is important to know that there are several complicated factors involved in these seemingly simple thermal imidization processes, which would determine the degree of imidization. The imidization reactions take place in a concentrated viscous solution (during initial and intermediate PAA stages), and the presence of residual solvent plays an important role during imidization at the later stages of the reaction. The chemical imidization is normally promoted by addition of organic bases such as pyridine and dehydrating agents, which is more susceptible to nucleophilic attack. Although the cyclodehydration reaction is allowed to proceed at 100 °C, the chemical imidization technique requires a final heat treatment (~200 °C) in order to remove the residual solvent completely [6]. Despite low energy requirements during the reaction, it is rarely used for applications due to the hazardous reagents involved.

One-step polymerization, as the name suggests, the intermediary PAA and PI are formed at the same time during reaction. This process involves a stoichiometric mixture of monomers in a high boiling solvent or in a mixture of solvents and reacts at 180–220 °C [7]. The imidization proceeds rapidly at high temperatures because of the azeotrope of generated water and solvent. In addition, the acidic catalyst such as benzoic acid is added in the first step to promote the formation of *trans*-isoimide. It has been proposed that a basic catalyst such as isoquinoline is necessary for converting the trans-isoimide into PI. Therefore, one-step polymerization process is especially useful for polymerization involving unreactive dianhydrides and diamines [8].

1.1.2. Modification of aromatic PIs

Even though the PIs have great potential for industrial applications owing to the outstanding thermal and mechanical properties, the utilization of aromatic PIs are restricted by the poor solubility due to the high crystallinity and stiffness of the polymer backbones, strong intermolecular interaction through π-π interaction, and charge transfer complex formation. For practical application, processability of plastics is the most important parameter in process engineering. Therefore, many scientists have strived on this project to prepare the organic soluble or thermoplastic PIs without sacrificing the desired thermal and mechanical properties. Various approaches of the chemical structure modification have been applied to improve the solubility and processability. Among these methods, the introduction of polar and kinked groups into the polymer chains is an effective method, such as aryl ether (—O—), ketone (—CO—), ester (—COO—), methylene (—CH_2—), and isopropylidene [—$C(CH_3)_2$—] into the polymer chains. In addition, the kinked groups not only form bent bonds but also lower the internal rotation energy of polymer chain, the packing effect of aromatic PIs has been weaken thus improve the solubility to organic solvents. Another approach is the replacement of symmetrical aromatic rings by asymmetrical structures, which will also decrease the packing efficiency and crystallinity between the polymer chains [9]. Moreover, the introduction of bulky pendant substituent along the polymer skeleton and kinked/non-coplanar structures into the polymer backbones can also reduce the packing order of chain, enhance the solubility, and disrupt crystallinity due to the random arrangement of substituent [10]. In summary, the aromatic PIs modified from the above mentioned approaches exhibit good solubility to organic solvents and amorphous property.

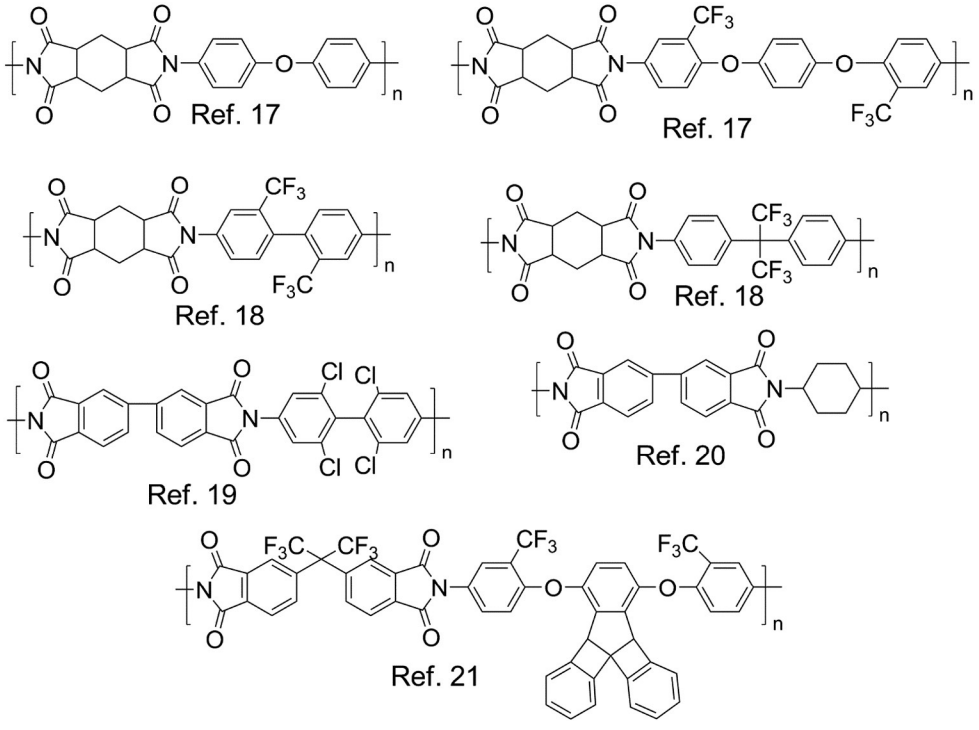

Scheme 1.2. Some High Optical Transparency Polyimides.

Please cite this article as: C.-L. Tsai, et al., Highly transparent polyimide hybrids for optoelectronic applications, Reactive and Functional Polymers (2016), http://dx.doi.org/10.1016/j.reactfunctpolym.2016.04.021

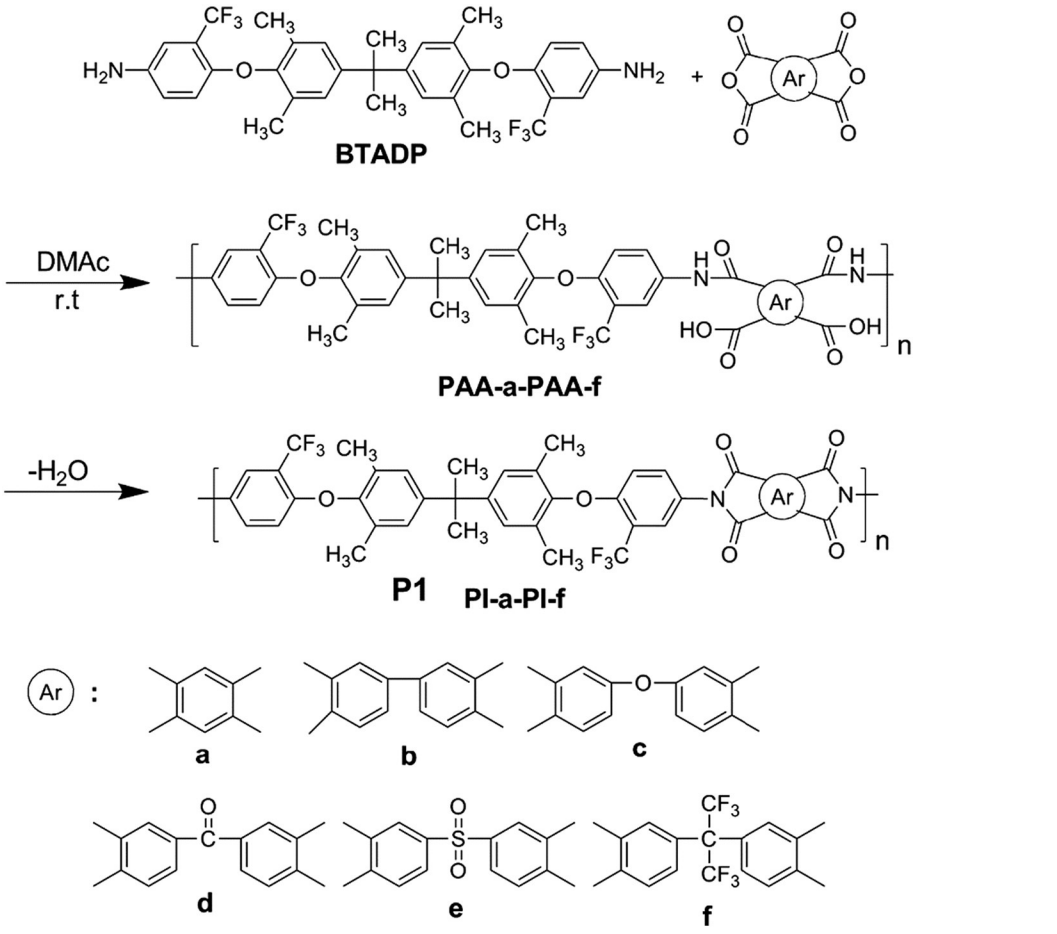

Scheme 1.3. Preparation of fluorinated polyimides (**P1**).

1.2. High optical transparency PIs

Aromatic PIs are well-known high performance polymers and good candidates for microelectronics and optoelectronic applications owing to their excellent properties, such as high thermal stability, good mechanical property, low dielectric constant and excellent chemical resistance [11]. However, one of the great disadvantages of the aromatic PI films for optoelectronic application is their yellowish nature. It is fully recognized that the commercial aromatic PI films, such as Kapton, give strong coloration from deep yellow to dark brown, which greatly limits the widespread application in areas where transparency and colorlessness are the basic needs [12]. In recent years, many efforts have been

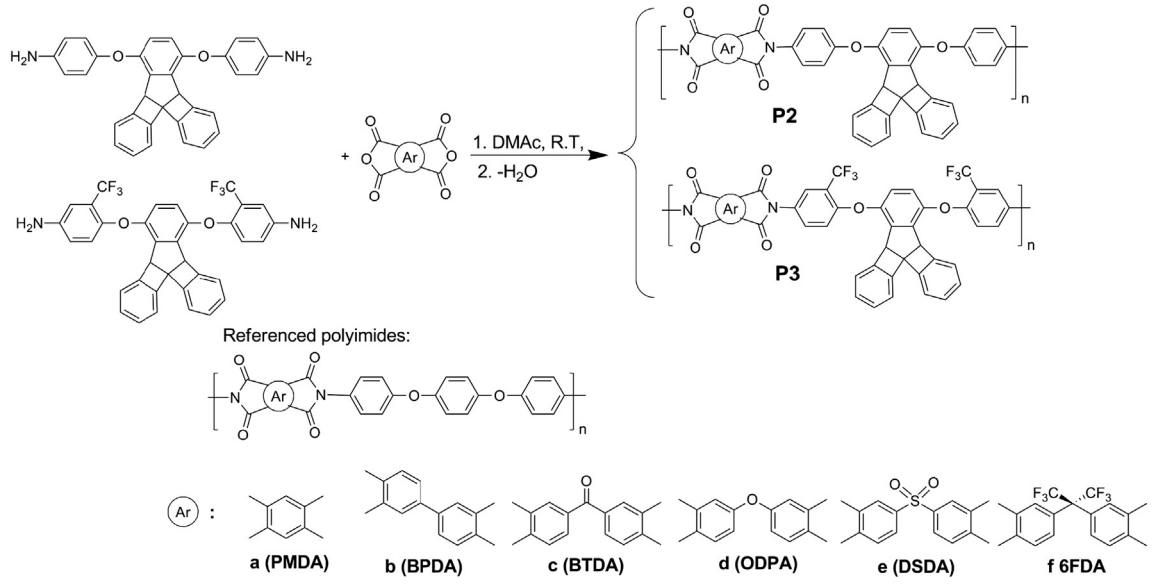

Scheme 1.4. Preparation of bulky triptycene-containing polyimides.

Please cite this article as: C.-L. Tsai, et al., Highly transparent polyimide hybrids for optoelectronic applications, Reactive and Functional Polymers (2016), http://dx.doi.org/10.1016/j.reactfunctpolym.2016.04.021

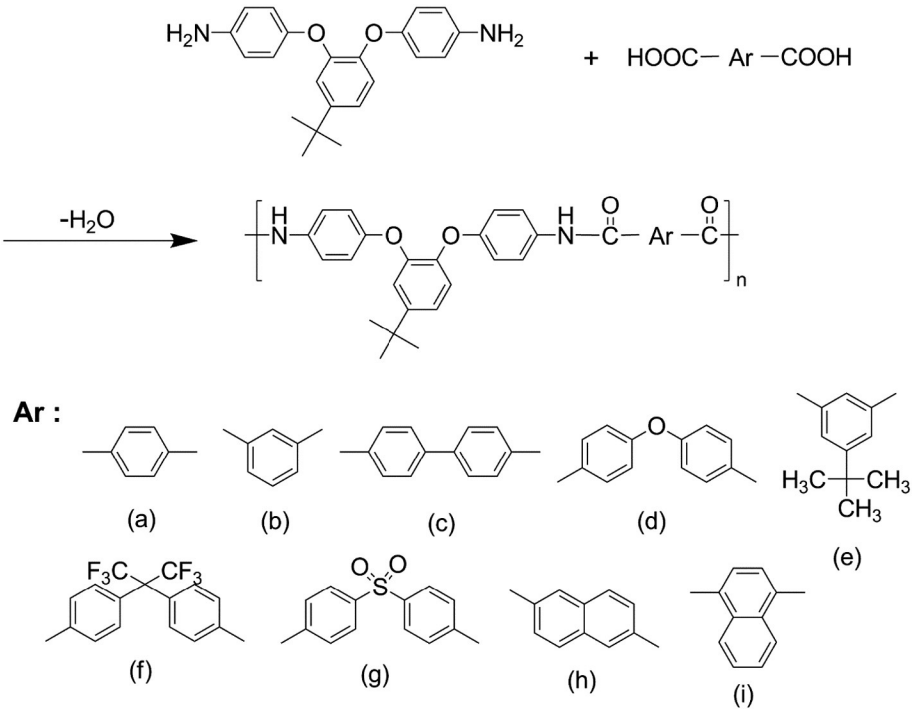

Scheme 1.5. Preparation of *ortho*- phenylene units and the *tert*-butyl group containing polyamides.

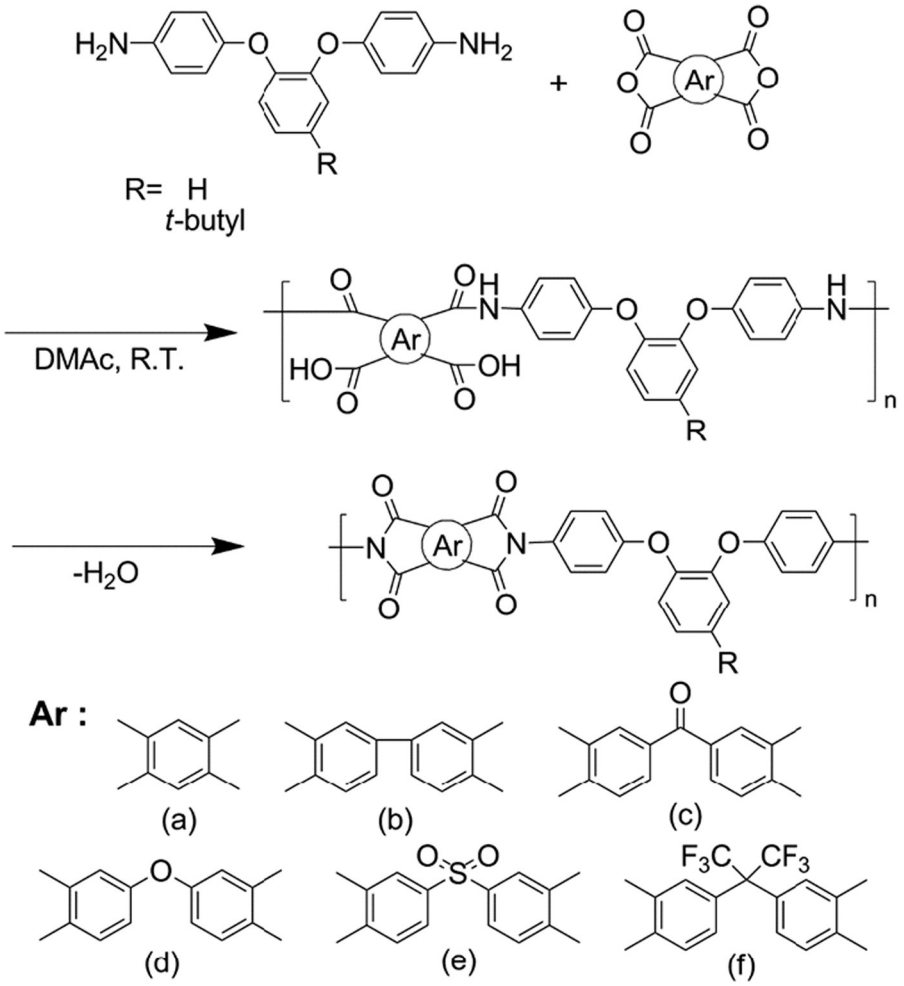

Scheme 1.6. Preparation of *ortho*- phenylene units and the *tert*-butyl group containing PIs.

Please cite this article as: C.-L. Tsai, et al., Highly transparent polyimide hybrids for optoelectronic applications, Reactive and Functional Polymers (2016), http://dx.doi.org/10.1016/j.reactfunctpolym.2016.04.021

made to develop highly optical transparent and colorless PI films along with high thermal stability and excellent mechanical properties for applications in prospective flexible electronic or micro-optical devices in the fields of displays, memory, lighting, solar cells, sensors, and waveguides [13]. In addition, optically transparent PI films also have potential uses in optoelectronic devices, flexible display substrates, and semiconductor applications [14].

It has been demonstrated that the original coloration in aromatic PIs is caused by the intra-/inter-molecular charge transfer complex (CTC) formation between the alternating electron-acceptor (dianhydride) and electron-donor (diamine) moieties. In this regard, the effective strategy for obtaining transparent and less-colored or colorless PIs is to use weak electron accepting dianhydrides or weak electron-donating diamines to suppress the charge transfer (CT) interactions [15]. In the past decades, many attempts have been made to improve the optical properties of PIs by incorporation of fluorine, chlorine, sulfone groups, or unsymmetrical and bulky pendent units, as well as adopting the alicyclic moieties in the polymer structure [16]. Some high optical transparency PIs are listed in Scheme 1.2 [17–21].

1.2.1. PIs containing unsymmetrical and bulky pendent units

Regarding the interlayer dielectrics, dielectric constant is a critical factor in minimizing electrical power loss and delay of signal transmission in thin-film insulators. Therefore, PIs with trifluoromethyl (—CF_3) or hexafluoroisopropylidene (6F) groups are of special interests, which will effectively increase the free volume and reduce the number of polarizable groups in a unit volume of the prepared PIs, thereby improves various properties such as solubility [22], optical transparency [23], and electrical insulating [14e].

A series of novel fluorinated PIs containing trifluoromethyl and tetramethyl substituents have been reported (Scheme 1.3) [24]. These PIs (**P1**) exhibited excellent solubility in organic solvents as well as high thermal stability and mechanical properties. The PI films also showed excellent mechanical properties, high optical transparency, and low dielectric constants. These characteristics indicated that fluorine-containing PIs are promising materials for optical applications.

Fluorinated PIs, in which fluorine atoms or —CF_3 groups are introduced into the polymer main chain or side chain, have been extensively investigated due to their unique characteristics. And previous research on fluorinated aromatic PIs demonstrated that the incorporation of bulky fluorine atoms or —CF_3 groups into the polymer structures resulted in an enhanced solubility and a lowered dielectric constant, as well as an improved optical transparency [25], which is attributed to their large free volume, low polarization of C—F bond and the high electron negativity [26]. Ando and Ha [19] developed the chlorine-containing aromatic PIs based on chlorinated diamines and found that the PIs exhibited good transparency, high refractive index and low birefringence due to the high polarizability of chlorine and the bulky molecular structure of the prepared chlorinated PIs.

St. Clair reported the aromatic PIs incorporated with bulky electron-withdrawing sulfonyl groups and indicated that the highly transparent PI films could be obtained because of the reduction of the inter-chain and intra-chain CTC formation [27]. The aromatic PIs with non-coplanar biphenyl structures and meta-substituted phenyl groups in the backbone, as well as the bulky pendant phenyl groups in the side chain have been studied by some researchers [28]. Hsiao's group also used the bulky triptycene pedant to decrease the charge transfer of the polymer chain (Scheme 1.4) [21]. It is also suggested that these PI (**P2**, **P3**) films have good solubility combined with high transparency, which can be attributed to the expanded free volumes and the weakened CTC formation. However, these aromatic polyimide films still have slight coloration due to the presence of CT interactions caused by the electron-donors and electron-acceptors from aromatic backbones.

The poly(ether-imide)s, having *ortho*-linked aromatic units in the main chain, have been reported that exhibit excellent properties including processability, either by solution or melt processing [29]. Recently,

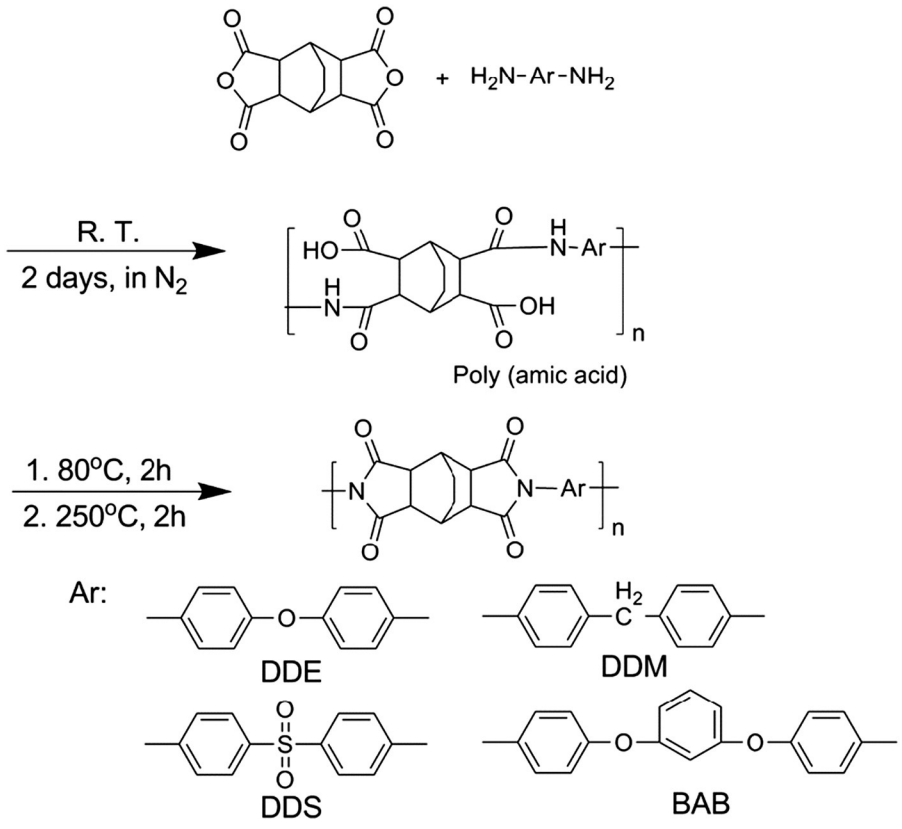

Scheme 1.7. Preparation of semi-aromatic polyimides.

Please cite this article as: C.-L. Tsai, et al., Highly transparent polyimide hybrids for optoelectronic applications, Reactive and Functional Polymers (2016), http://dx.doi.org/10.1016/j.reactfunctpolym.2016.04.021

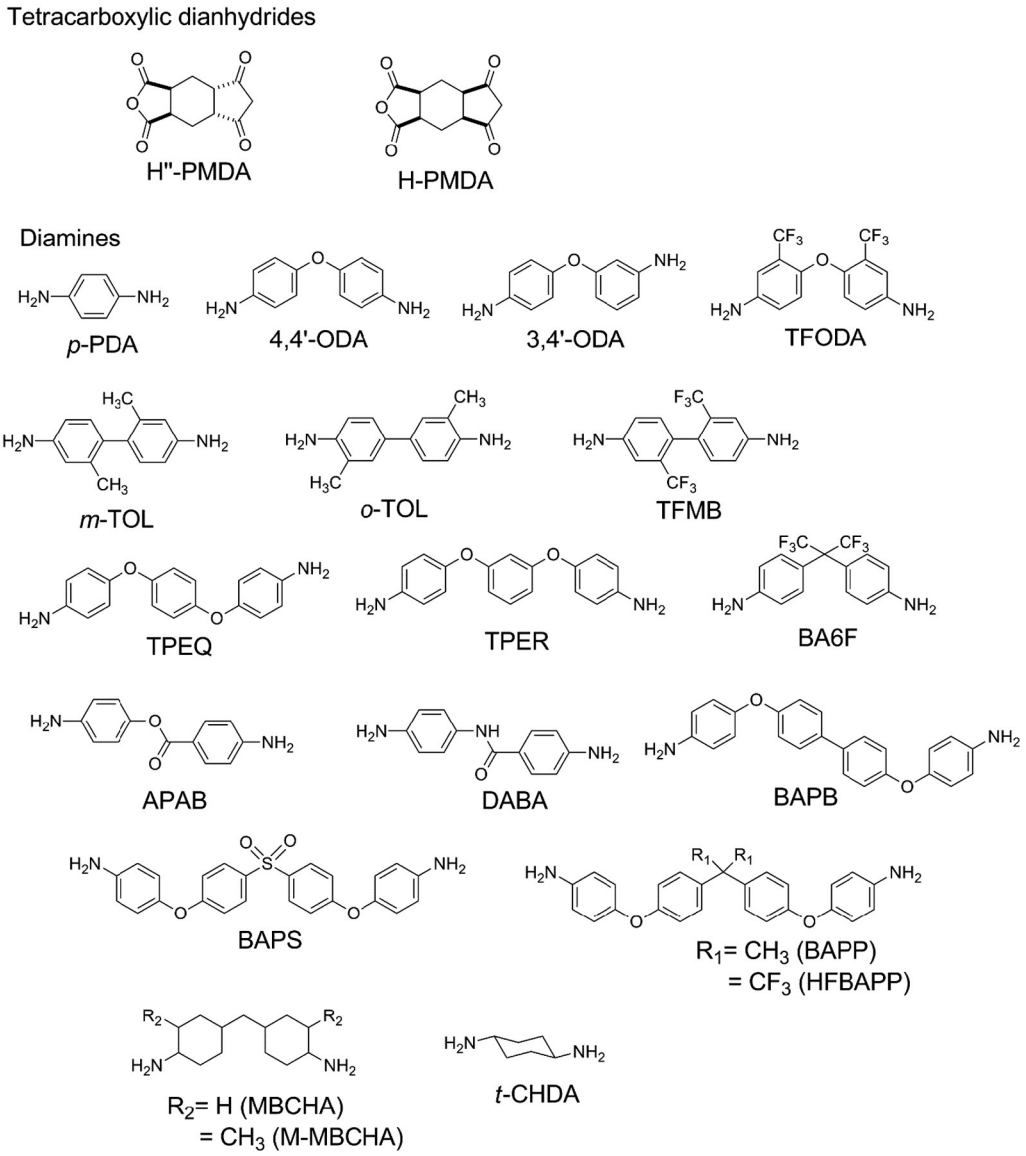

Scheme 1.8. Molecular structures of the diamines and dianhydrides.

Hsiao et al. have demonstrated that the combination of *ortho*-phenylene units and the *tert*-butyl group could further improve processability and film toughness in polyamides [30] (Scheme 1.5) and PIs [31] (Scheme 1.6).

1.2.2. PIs containing alicyclic monomers

Non-aromatic PIs derived from dianhydrides and/or diamines with alicyclic structures have been developed by Matsumoto [32] and other researchers [33]. It is suggested that the non-aromatic PIs displayed good solubility, low dielectric constant and high transparency, which is due to their relatively lower molecular density and polarity, especially the absence or inhibition of intra- and/or inter-molecular CT interactions [34]. Therefore, the incorporation of alicyclic units in PIs is considered as one of the effective ways to enhance the transparency in the UV–visible region and other desired properties. Unfortunately, the fully alicyclic PIs prepared from alicyclic dianhydrides and diamines possess

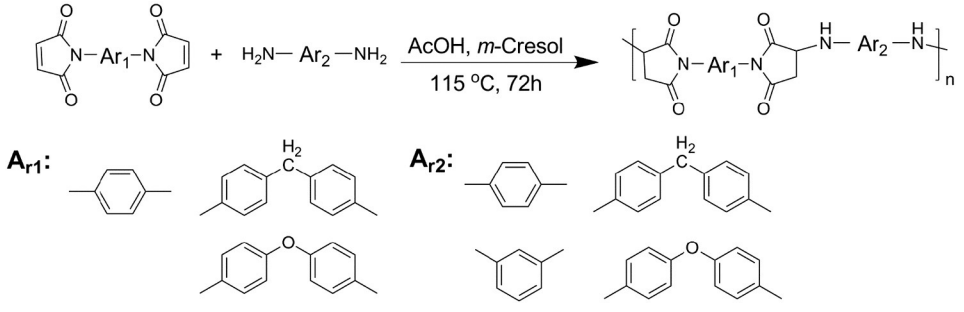

Scheme 1.9. Preparation of polyaspartimides.

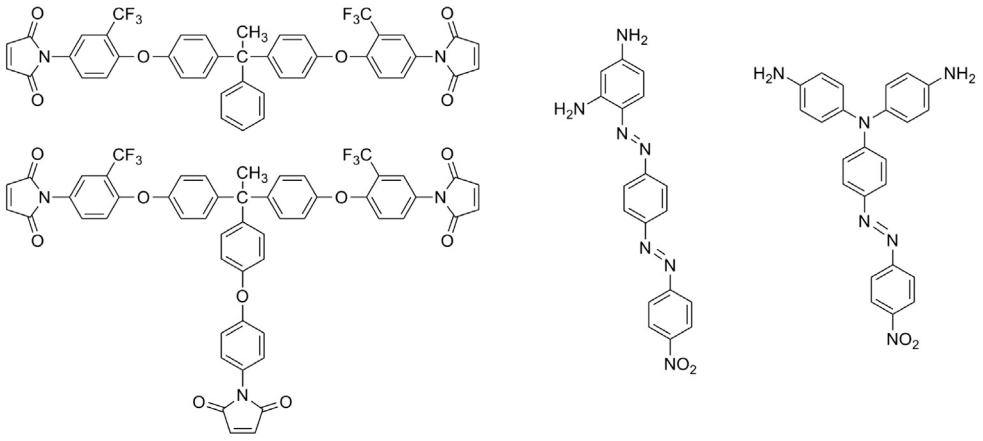

Scheme 1.10. Chemical structure of the trimaleimide, bismaleimide and azobenzene dye monomers.

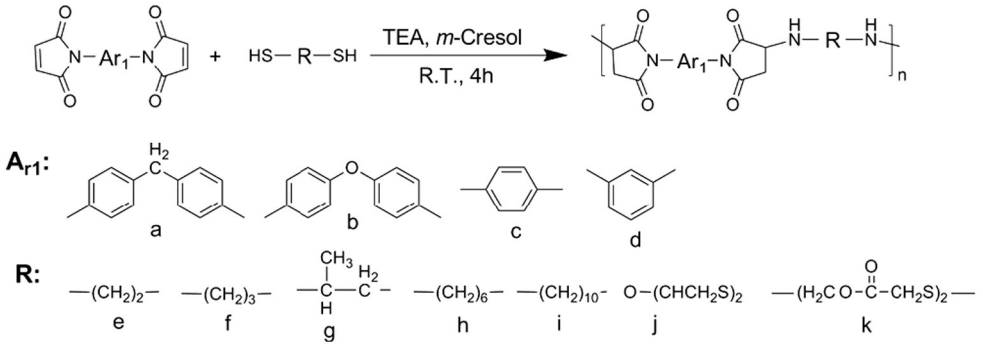

Scheme 1.11. Michael polyaddition of the polyimidothioethers.

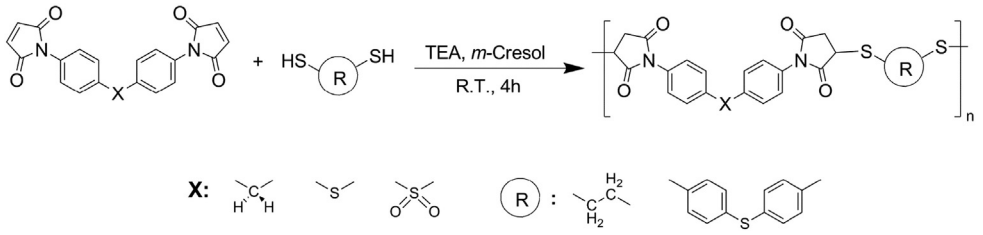

Scheme 1.12. Synthesis of the Polyimidothioethers.

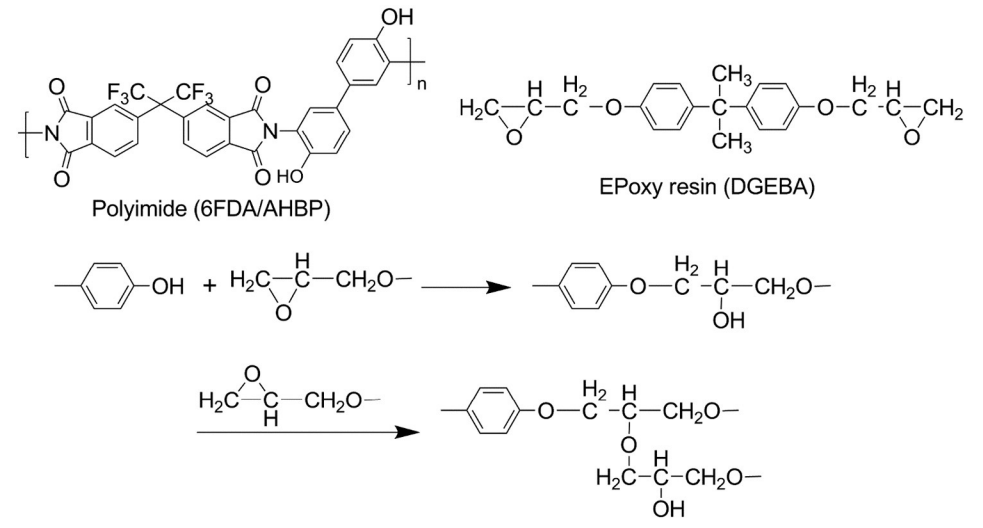

Scheme 1.13. Reaction profile of epoxy resin with the reactive polyimide.

Please cite this article as: C.-L. Tsai, et al., Highly transparent polyimide hybrids for optoelectronic applications, Reactive and Functional Polymers (2016), http://dx.doi.org/10.1016/j.reactfunctpolym.2016.04.021

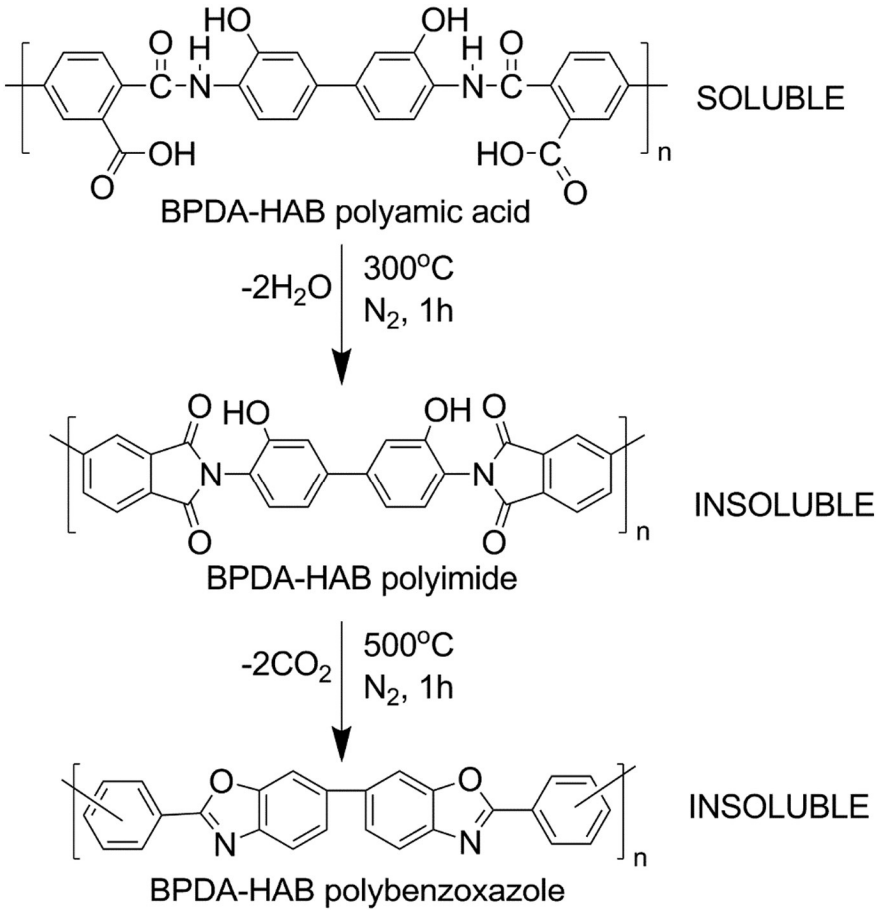

Scheme 1.14. Thermal imidization of BPDA-HAB polyamic acid at 300 °C and subsequent thermal conversion to aromatic polybenzoxazole at 500 °C under nitrogen.

much lower thermal stability than the corresponding fully aromatic PIs, which is a major drawback for practical application. In order to improve thermal stability of alicyclic PIs, the semi-aromatic PIs derived from aromatic dianhydrides/alicyclic diamines or alicyclic dianhydrides/aromatic diamines were then developed (Scheme 1.7) [35].

Recently, the semi-aromatic PIs prepared from alicyclic dianhydrides and aromatic diamines have more attracted due to their highly transparency without sacrificing thermal stability and mechanical toughness, which make them good candidates for applied as colorless and transparent substrates.

Ueda's group have succeeded the synthesis of semi-alicyclic PI with a high molecular weight based on aliphatic diamine (*trans*-1.4-cyclohexanediamine, *t*-CHDA) and aromatic dianhydride by the addition of acetic acid [36]. After that, Hasegawa's group has developed a series of high molecular weights semi-alicyclic PIs based on aliphatic diamines and dianhydrides (Scheme 1.8) [18]. Thus, the salts formed from aliphatic or alicyclic diamines and monocarboxylic acids have higher solubility in organic solvents than those salts formed from aliphatic or alicyclic diamines and PAAs [36,37].

1.2.3. Bismaleimide-type PIs

It is also well known that thermosetting PIs derived from bismaleimides (BMIs) exhibit excellent thermal and mechanical properties, thus making them extremely popular for advanced composite and electronics. BMIs can be self-polymerized through their reactive maleic double bonds to give highly cross-linked, rigid, and brittle PIs. On the other hand, nucleophilic difunctional reagents such as diamines and dithiols could react with the strongly electrophilic maleic double bonds to afford linear and high-molecular-weight PIs. In particular, diamines have been used to extend BMIs, resulting in polyaspartimides and polyimidothioethers (PITEs). Crivello [38] reported a detailed investigation of the condensation of aromatic amines and maleimide in 1973 (Scheme 1.9). White and Snider [39] then compared the reactions of the secondary diamines with BMIs via Michael polyaddition. Recently, new linear polyaspartimides were obtained via Michael addition from several functional diamine-based BMIs with various aromatic diamines in *m*-cresol [40]. These polymers exhibited an amorphous morphology with good solubility, high T_g values, and good thermal stability, which could be considered to be new processable polymeric materials.

Through the Michael addition, thermally stable nonlinear optical (NLO) hyperbranched systems consisting of azobenzene dyes have been successfully synthesized (Scheme 1.10) [41]. All of the obtained polymers were soluble in DMF, DMAc, and DMSO. The thermal stability was greatly enhanced by incorporating the polyaspartimide structure into the NLO-active hyperbranched polymers. All the hyperbranched polymers exhibited better NLO properties than their corresponding linear analogues due to the presence of a spherical shape and site isolation effect. Moreover, waveguide properties could be also achieved for all the NLO polymers.

Table 1.1
Electronegativity (χ), Coordination Number (N), and Degree of Unsaturation (N-Z) of Some Metals (Z = 4).

Alkoxides	χ	N	N-Z
$Si(OPr^i)_4$	1.74	4	0
$Sn(OPr^i)_4$	1.89	6	2
$Ti(OPr^i)_4$	1.32	6	2
$Zr(OPr^i)_4$	1.29	7	3
$Ce(OPr^i)_4$	1.17	8	4

Please cite this article as: C.-L. Tsai, et al., Highly transparent polyimide hybrids for optoelectronic applications, Reactive and Functional Polymers (2016), http://dx.doi.org/10.1016/j.reactfunctpolym.2016.04.021

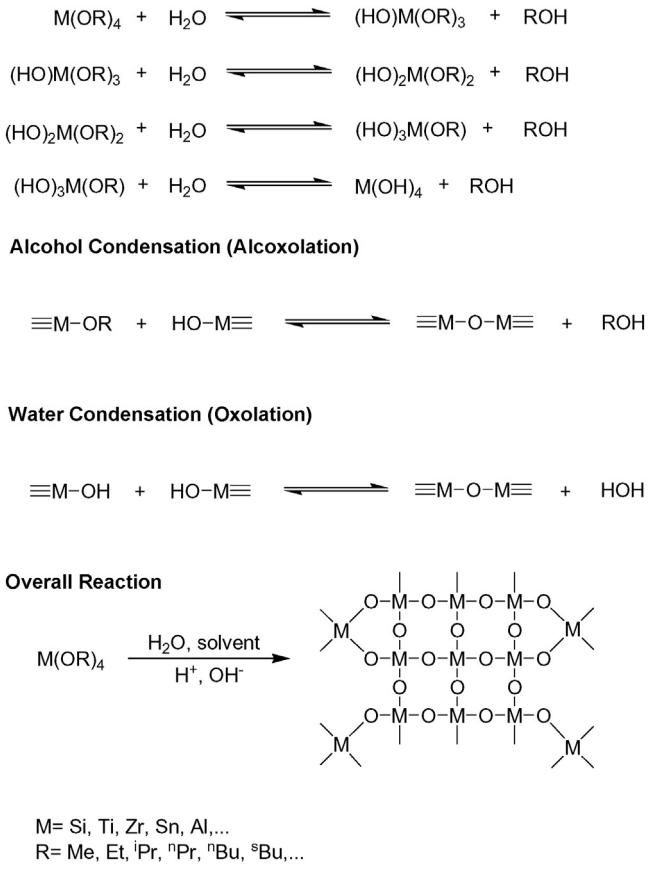

Scheme 1.15. Forming frameworks of metal oxide by hydrolysis and condensation reactions.

The condensation of maleimide compounds with hydrogen sulfide and bisthiols was studied in several model systems by Crivello [42] in 1976 (Scheme 1.11). BMI compounds undergo rapid, exothermic polymerization with thiol-containing compounds in *m*-cresol and basic catalyst to give linear PITEs with high viscosity. PITE copolymers can readily be prepared by mixing two BMI monomers together in solution and then adding a catalyst and hydrogen sulfide. Random copolymers were obtained in this manner and revealed properties as a combination of those of the two homopolymers; they exhibited only one glass transition temperature and one melting point.

Liou's group [43], therefore, used this facile approach to prepare a series of thermoplastic PITEs (Scheme 1.12), which were highly soluble in various organic solvents and showed useful thermal stability associated with high glass transition temperatures. These optically isotropic thermoplastic PITEs exhibiting well-balanced optical properties are promising candidates for optical waveguide or encapsulant materials in advanced optical applications for both solution casting and injection molding techniques.

1.3. Functional organic-inorganic hybrid nanocomposites

Organic-inorganic hybrid materials have attracted considerable attention in recent years due to their novel physical and chemical properties. The sol-gel process in preparing inorganic/organic hybrid materials has been used by several researchers. The various characteristics of the sol-gel process, such as metal-organic precursors, organic solvents, low processing temperature, and the processing versatility of colloidal states, allow the mixing of inorganic and organic components at the scales ranging from Angstrom to nanometer. By tailing the organic and inorganic moieties into nanosized domains, they can produce nanostructured materials with novel physical and chemical properties. Therefore, the presented advantages for designing materials lead to the so-called "functional hybrid organic-inorganic nanocomposites" [44]. The nature of the interface between organic and inorganic components has been used recently to classify these hybrids into two different classes [45]. Class I corresponds to all the systems in which there are no covalent or ionic covalent bonds between the organic and inorganic components. There are only Van der Waals forces, hydrogen bonds, or electrostatic forces between them. In contrast, some of the organic and inorganic components are linked through strong chemical bonds (covalent or ionic-covalent), which are defined as class II materials. The construction of the hybrid networks depends on the relative stability of the chemical links that associate the different components. The interfacial force between organic and inorganic phases plays a major role in controlling the microstructure and properties of composite materials [46]. The most obvious advantages of organic-inorganic hybrids are that they can favorably combine the unique properties of organic and inorganic components in one material. Briefly, the organic components allow easy shaping and better processing. The inorganic components can provide mechanical, thermal stability, implement or improve electronic, magnetic and redox properties, density, refractive index, etc.

Table 1.2
The reaction constant K of tetralkoxysilane hydrolysis in acid.

R	$k\ 10^2$ (1 mol^{-1} s^{-1} $[H^+]^{-1}$)
C_2H_5	5.1
C_4H_9	1.9
C_6H_{13}	0.83
$(CH_3)_2CH(CH_2)_3CH(CH_3)CH_2$	0.30

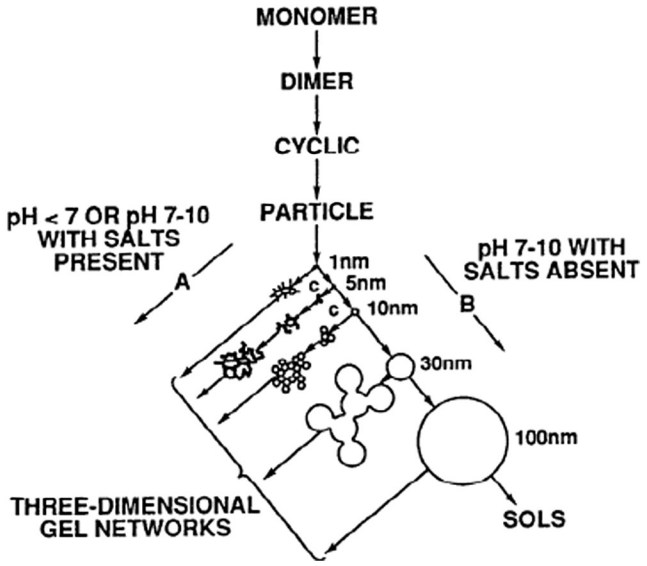

Fig 1.1. Reaction behavior of metal alkoxides.

1.3.1. PI containing hydroxyl groups

The hydroxyl-containing PIs were expected to result in interesting and potentially useful properties, e.g., high glass transition temperatures (T_g), the thermal stability for photoresist [47], and nonlinear optical (NLO) applications [48]. The pendant hydroxyl groups on the backbones of the imidized PIs were important to ensure the solubility and the reactive sites for subsequent condensation reactions. Marks and co-workers [49] achieved a second-order NLO material system of polyfunctional epoxide and diisocyanate cross-linked chromophoric poly(hydroxystyrene)s with high T_g. Takeichi et al. (Scheme 1.13) [50] developed the hydroxyl-containing side-chain PIs can be used as reactive PIs and cross-linked with polyurethane prepolymers or epoxy resins to improve the mechanical properties, solvent resistance, and thermal stability of the materials. Tullos et al. [51] reported that aromatic PIs containing hydroxyl groups

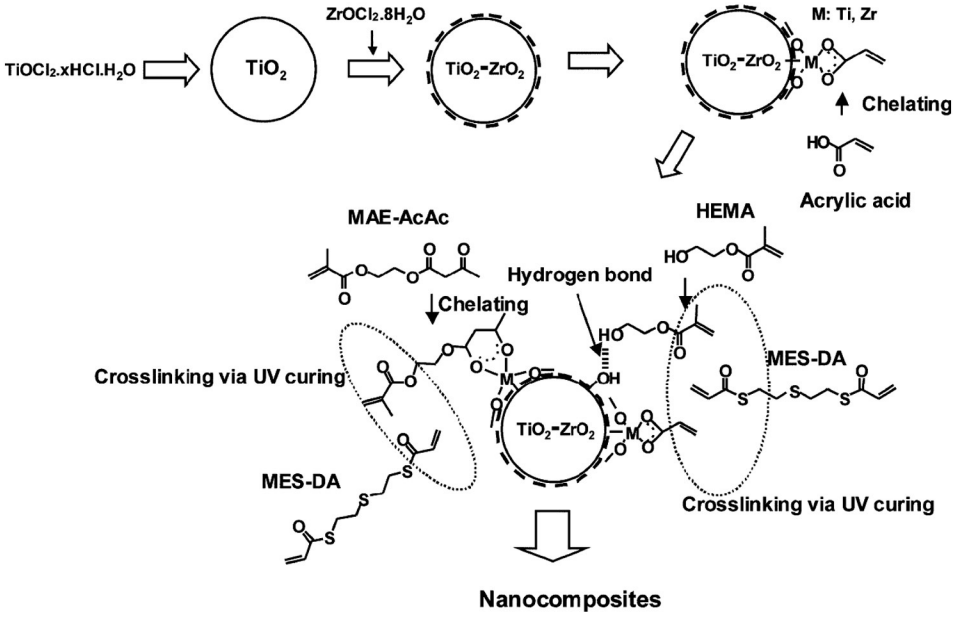

Scheme 1.16. Schematic representation of mechanism to fabricate the nanocomposites via UV-induced crosslinking polymerization.

at the *ortho*-position to the imide nitrogen could undergo thermal conversion to polybenzoxazoles upon heating between 350 and 500 °C under nitrogen or vacuum accompanied by loss of carbon dioxide (Scheme 1.14).

1.3.2. Sol-gel chemistry

Considering the key role in the preparation of organic-inorganic hybrid materials, sol-gel chemistry has greater flexibility in process technology with excellent thermal stability and optical transparency.

The sol-gel method was first developed by Ebelmen [52], who prepared the metal alkyloxide from ethanol and $SiCl_4$. About a century later, Geffcken manufactured the oxide film from alkoxyphenyl materials, this material was caught extensively the world's attention [53]. Hurd pointed out that the network structure was polymerized from the backbone of silica acid around the continuous liquid phase, the consideration makes the concept of network structure accepted [54]. In 1990, McGrath and coworkers connected the low molecular weight PI to the network [55], and generated sol-gel organic-inorganic composite materials, leading sol-gel chemistry as multifunctional materials for future application [56].

Sol-gel process is based on nucleophilic reactions, involving hydrolysis and condensation reactions. The hydrolysis reaction is due to the higher electronegative alkoxy groups with the combination of electron-

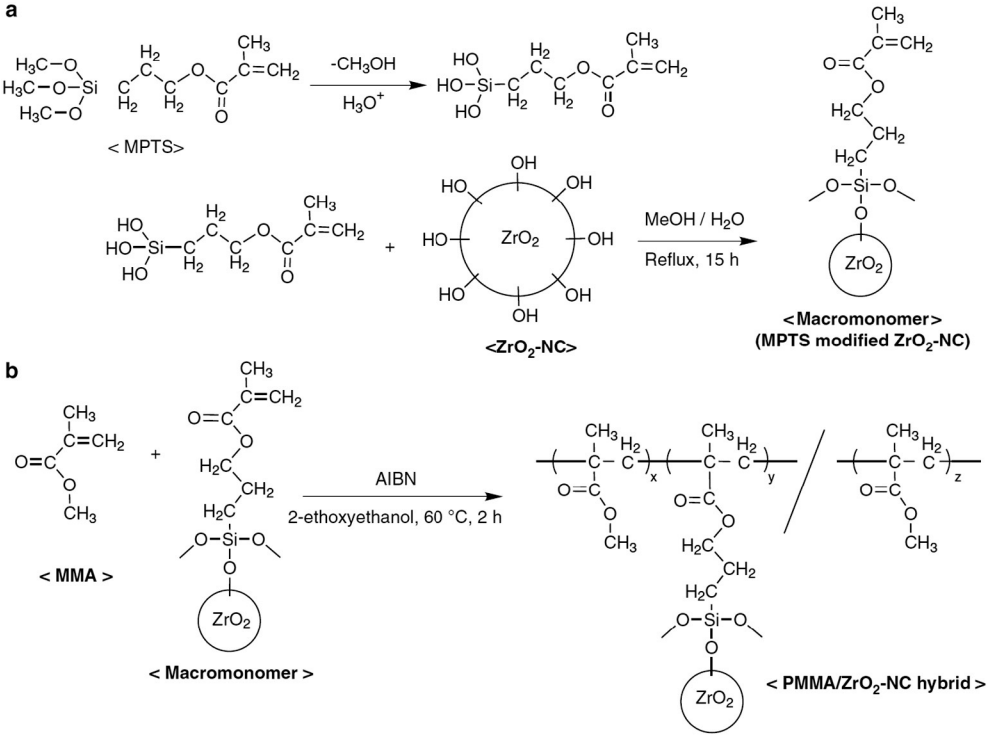

Scheme 1.17. Reaction route for preparing (a) 3-(methacryloxy)propyl-trimethoxysilane (MPTS)-modified zirconium oxide nanocrystals (ZrO2-NCs) as macromonomers and (b) poly(methyl methacrylate) (PMMA)/ZrO2-NC hybrid materials.

Please cite this article as: C.-L. Tsai, et al., Highly transparent polyimide hybrids for optoelectronic applications, Reactive and Functional Polymers (2016), http://dx.doi.org/10.1016/j.reactfunctpolym.2016.04.021

Table 1.3
Examples for AgNWs-high performance polymer hybrid systems.

Substrate type	Aspect ratio of AgNWs	R_s (Ω/sq)	$T_{550\ nm}$ (%)	FoM	Notes	Ref
Commercial PI[a]	1000	15	90	230	Transferring Heater	[78a]
Commercial PI[b]	500	12	85	180	Hybrid with ITO Brush coating Solar cell	[78f]
Commercial PI[c]	375	21	85	105	Spin coating Solar cell	[78g]
Commercial PI[c]	350	30	89	105	Rod casting Pulse light sintering	[78h]
MDPB-FGEEDR copolymer	300	9.5	50	50	Drop casting Transferring	[78b]
6FOH-ODPA PI	250	-[c]	–	–	Spray coating	[78e]
Commercial PI[d]	150	–	–	–	Drop coating	[78c]
TFMBCH PI	215	5.6	58	105	Spin coating Transferring	[78i]

[a] Product model of commercial PI: VTEC-080051.
[b] The commercial PI is supplied by Kolon Industry, LTD.
[c] Not mentioned.
[d] The commercial PI is supplied by Evonik, Germany.

withdrawing metal ions, leading to metal ions into the electrophilic-center for nucleophilic attack. The chemical reactivity of the metal alkoxide in the hydrolysis step is determined by both the nature of the metal, M, and the steric hindrance of the alkoxy groups. The major parameters appear to be the electrophilic character of the metal atom (electronegativity, χ) and its ability to increase the coordination number (N). The unsaturation degree of the metal coordination can be expressed by the difference N-Z, (oxidation state, Z). Table 1.1 lists the values for various metal alkoxides [57]. This process starts with molecular precursors at ambient temperatures, forming metal oxide frameworks by hydrolysis and condensation reactions (Scheme 1.15).

Where R is an alkyl group, C_nH_{2n+1}, which will be the obstacles to the hydrolysis and condensation reactions. R-based branched-chain and the longer main chain show the slower the hydrolysis rate as depicted in Table 1.2 [58], and subsequent condensation reactions involving the M-OH produce M-O-M and alcohol (ROH) or water. Because water is produced as a by-product of the condensation reaction, and γ value (H_2O: M molar ratio) of 2 is theoretically sufficient for complete hydrolysis and condensation to yield anhydrous silica. The chemistry of metal alkoxides, the catalysts, the H_2O: M ratio, the solvent effects, the reaction temperature are the main factors to control the resulting structures [59].

For the common metal alkoxides, the reaction rate depends strongly upon the catalysts. In an alkaline environment (pH = 7–10), the condensation reaction rate is faster than hydrolysis, according to Ostwald ripening mechanism, the particles grow, prepared by the system of mass fractal dimension is greater; on the contrary, under acidic conditions, condensation rate is slower than the hydrolysis, and the particle growth results in aggregation of small particles which will create a mass fractal dimension product of relatively small structures as shown in Fig. 1.1 [60].

1.3.3. Titania-based hybrid nanocomposites

Titanium alkoxides $Ti(OR)_4$ are in general very reactive due to the presence of highly electronegative —OR groups that stabilize titanium in its highest oxidation state and render titanium very susceptible to nucleophilic attack. It is a non-toxic, wide band gap semiconductor and can be categorized to three crystal structures, anatase, rutile and brookite. Experimental results have shown that the prepared TiO_2 photocatalyst thin film can overcome the disadvantages of its powder shape and to extend the industrial applications, such as, used as antibacterial ceramic tile and self-cleaning glass [61]. It is due to the excellent photocatalytic properties as well as the high transparency, excellent mechanical and chemical durability of TiO_2 films in the visible and near-infrared region of the spectrum. Among these properties, the most interesting object is mainly focusing on the high-refractive-index property of titania. Therefore, many kinds of polymers such as poly(methyl methacrylate) [62], polyimide [63], poly(silsesquioxanes) [64], and others [65] have been incorporated with titania.

Table 2.1
Comparisons of Organic and inorganic Materials.

Materials	Advantages	Disadvantages
Organic	Low density (1.0–1.5)	Low RI
	Easy to fabricate	Low Abbe number
	Low cost	Relatively thermally unstable
Inorganic	High RI	High density (2.2–3.0)
	High Abbe number	Brittle
	Good thermal properties	Expensive

1.3.4. Zirconia-based hybrid nanocomposites

Transparent inorganic oxides such as TiO_2 and ZrO_2 (zirconia) possess refractive indices higher than 2 in the visible (e.g., bulk refractive indices of 2.55 and 2.10 for TiO_2 and ZrO_2 (at 589 nm), respectively), which are much higher than those of available monomer and polymeric binder materials. In an attempt to produce the inorganic-organic nanocomposites having high refractive index, high transparency and good mechanical properties, Nakayama and Hayashi carried out the following approach. First, the TiO_2-ZrO_2 nanoparticles were synthesized by using ZrO_2 as an outer layer of TiO_2 nanoparticles to depress the photocatalytic activity of TiO_2 [66]. Then, the surface of the nanoparticles was modified by acrylic acids to control the aggregation between the nanoparticles, and the nanocomposites could be obtained with photo-crosslinkable materials by UV curing methods (Scheme 1.16).

ZrO_2 is an important material due to its superior hardness, high refractive index, and high transparency in the visible and near-infrared region, chemical stability and low thermal conductivity. Especially, ZrO_2 has a low dispersion of refractive index due to its large band gap energy. These unique properties of ZrO_2 have led to their widespread applications in the field of optical, structural materials and thermal barrier coatings [67].

Otsuka and Chujo prepared high transparent and homogeneous hybrids containing a single nano-sized inorganic oxide domain, which were synthesized from poly(methyl methacrylate) (PMMA) and aqueous dispersed zirconium oxide nanocrystals (ZrO_2-NCs) in the presence of a coupling agent, 3-(methacryloxy)propyl-trimethoxysilane (MPTS), which was grafted onto the surface of ZrO_2-NCs by zirconium hydroxide (Zr-OH) surface groups [68]. The surface-functionalized ZrO_2-NCs were used as macromonomers in the process of grafting from polymerization of methyl methacrylate (MMA). The densities of surface Zr-OH groups

Please cite this article as: C.-L. Tsai, et al., Highly transparent polyimide hybrids for optoelectronic applications, Reactive and Functional Polymers (2016), http://dx.doi.org/10.1016/j.reactfunctpolym.2016.04.021

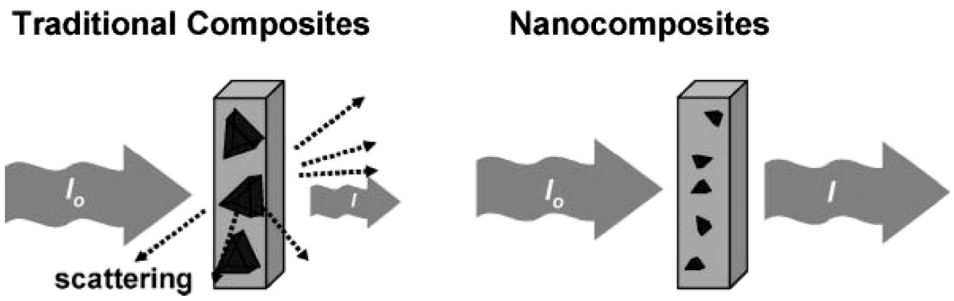

Fig 2.1. Decreasing the size of inorganic particles allows for the functionalization of transparent polymers without significant loss of transparency if the particles are isolated from each other inside the polymer matrix.

and MPTS surface modifications were determined using thermogravimetric analysis. Hybrid films retained good optical transparency because of the formation of nanometer miscibility and good affinity between PMMA and ZrO_2-NCs compared with that of PMMA/ZrO_2-NC blend composites. Owing to their excellent optical properties and high thermal stability, PMMA/ZrO_2-NC hybrids have great potential for application in optical and mechanical fields (Scheme 1.17).

1.3.5. AgNws/polymers Nanocomposites

Although ITO has occupied most of the market of transparent electrode for its excellent properties in electric and optical behavior, however, high cost and brittle property are the crucial problems need to face with. Owing to the advance in technology, the requirements of transparent electrode such as stretchability, flexibility, and bendability have been taken into considerations. Thus, ITO system is no longer the most popular material in this field due to the brittleness even coated on flexible substrates.

Metallic nanowire is a good candidate of transparent and conducting materials. Among the metal nanowires, silver nanowire (AgNWs) are the most popular materials and exhibits a great potential to enhance the conductivity of transparent film by tuning the aspect ratios and containing concentration due to the highest electrical conductivity. For example, the loading of silver in polymeric composites could be greatly reduced if nanoparticles were replaced by nanowires with higher aspect ratios [69].

To highlight the advantages of AgNWs, the first AgNWs-polymer (PET) hybrid flexible electrode has been prepared by Coleman's group [70]. However, the poor adhesion property of AgNWs between substrate is a crucial problem and became a primary issue that many scientists tried to solve it. For example, the introduction of additional encapsulation material or changing suitable substrate is a good approach that presented by Zhou's and Cui's groups [71].

Table 2.2
Refractive Indices of Polymers from Sulfur-Containing Aliphatic and Alicyclic Methacrylate.

Monomer	Refractive index	Abbe number	Entire light transmittance (%)
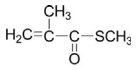 (MTMA)	1.582	38.6	91
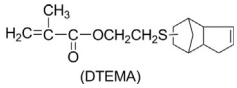 (DTEMA)	1.557	47.4	91
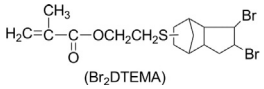 (Br_2DTEMA)	1.612	31.0	90
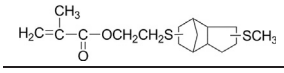	1.580	50.0	90

Furthermore, another polymeric substrate such as polydimethylsiloxane (PDMS) [72], polyacrylate [73], polyurethane (PU) [74], poly(methyl methacrylate) (PMMA) [75], polycarbonate (PC) [76], and polyvinyl alcohol (PVA) [77] have joined the family of AgNWs hybrid electrode and provided all kinds of impressive properties. For example, the stretchable AgNWs electrode was prepared by introducing PDMS as the substrate owing to their excellent stretchability, toughness, and flexibility as well as the stronger adhesion to AgNWs than other flexible substrate. Moreover, the advantages of AgNWs such as mechanical properties (ductility, bendability) have been also highlighted. Most of the AgNWs are buried in the PMDS by transferring or pasting method from glass substrate, and the low sheet resistance and surface roughness is a strong indication that diffusion of electrons in AgNWs coating layers did not interrupt by polymer matrix.

Although many researches of AgNWs-polymer electrode mentioned above have reached high performance on optical and electrical properties, the thermal stability of theses polymers are still not good enough for practical usages to endure higher temperature processing or long-term harsh environments. It is good approach to introduce high performance PI or other thermal setting polymer into AgNWs systems, but just few researches focus on this method due to the difficult synthetic steps (Table 1.3) [78].

The requirement of thermal stability on AgNWs flexible electrode was first mentioned by Kim's group and applied in solar cell devices till 2012 [78g]. They also investigated the mechanical properties of the AgNWs network electrodes coated on colorless PI by outer/inner, twisting and stretching test system. Moreover, higher FoM value (180) of AgNWs-PI film was achieved by same group in 2013 [78f]. Owing to the combination of ITO layer and AgNWs networks, the brittleness ITO layers have been improved. However, it is a pity that the optical and thermal properties of AgNWs-PI haven't been investigated completely. The cut-off wavelength of PI substrate adopted in AgNWs system is still high due to the coloration by CTC formation. Therefore, it is necessary to highlight the advantages of high performance polymer by advanced structural design and preparation of AgNws/polymers nanocomposites.

Table 2.3
Structure and Refractive Index of Episulfide Monomer and Diisocyanate.

Structure of episulfide monomer and diisocyanate	Refractive index
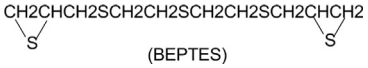 (BEPTES)	1.635
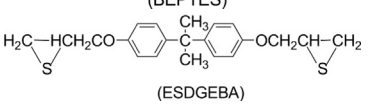 (ESDGEBA)	1.61
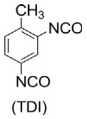 (TDI)	1.567

Please cite this article as: C.-L. Tsai, et al., Highly transparent polyimide hybrids for optoelectronic applications, Reactive and Functional Polymers (2016), http://dx.doi.org/10.1016/j.reactfunctpolym.2016.04.021

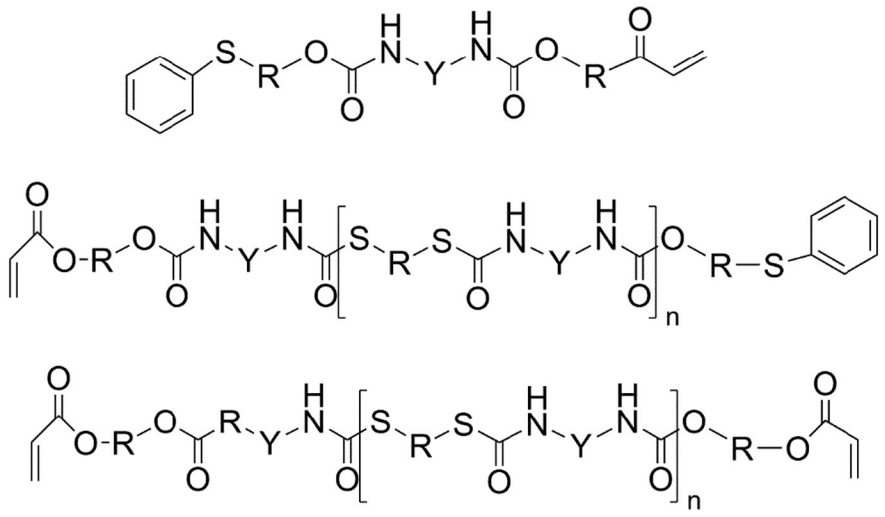

Scheme 2.1. Generic structures of prepared thiourethane acrylates. Y stands for aromatic group, R stands for alkyl.

2. Highly transparent PI hybrids for optical applications

2.1. High optically transparent and refractive hybrid materials

High refractive index (RI) polymers have been developed in recent years due to the increasing demands for advanced optical applications [79]. It has been well accepted that the performance of the optical devices can be improved by utilizing high RI materials, such as high performance substrates for advanced display devices [80], optical adhesives or encapsulants for organic light-emitting diode devices (OLED) [81], antireflective coatings for advanced optical applications [82], and micro-lens components for charge-coupled devices (CCD) [83].

Inorganic materials usually have a high RI (in the range of 2.0–5.0) [84]. However, they have disadvantages including higher densities and lower flexibility. Particularly, for the fabrication of antireflective coatings, the RI of inorganic materials cannot be tuned continuously and the fabrication procedures are becoming more complex and expensive.

Organic-inorganic hybrid materials can be potential candidates for high RI materials, which combine the advantages of the organic polymers (lightweight, flexibility, good impact resistance, and good

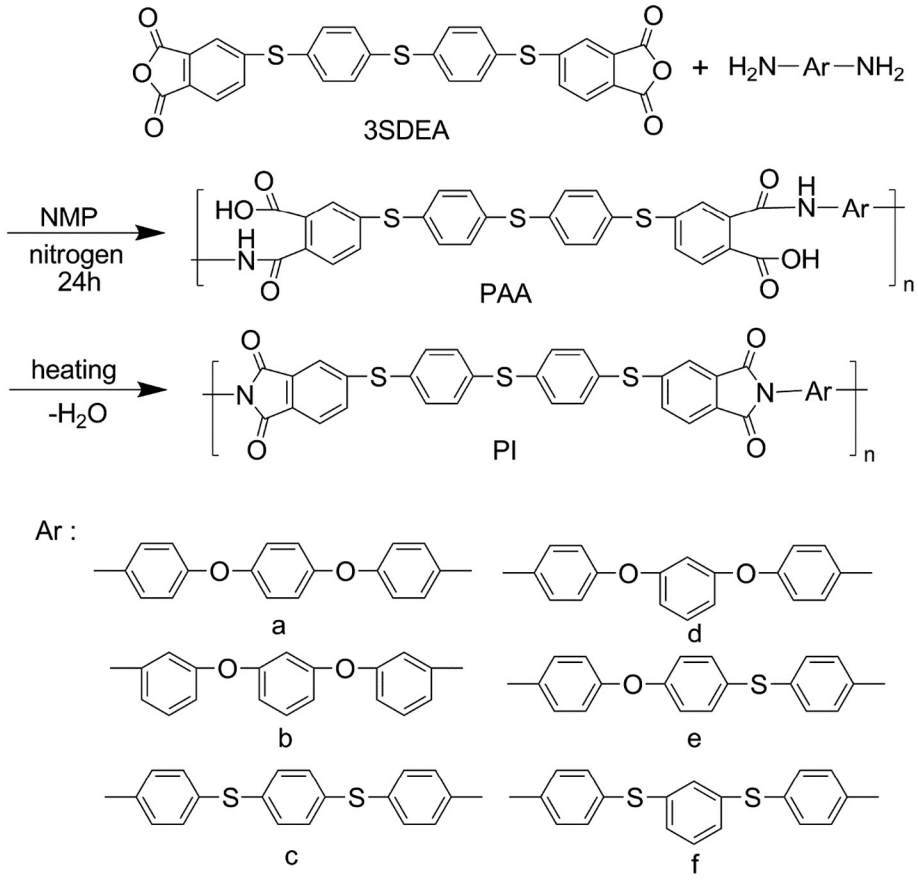

Scheme 2.2. Synthesis of PIs.

Please cite this article as: C.-L. Tsai, et al., Highly transparent polyimide hybrids for optoelectronic applications, Reactive and Functional Polymers (2016), http://dx.doi.org/10.1016/j.reactfunctpolym.2016.04.021

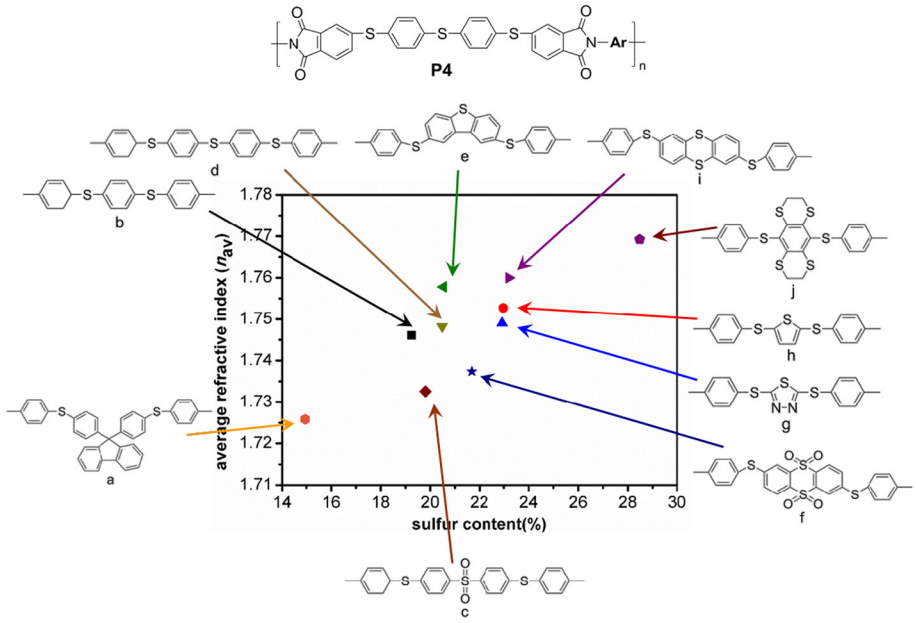

Fig 2.2. The refractive index increased with increasing sulfur content of the PIs by Ueda group.

processability) and inorganic materials (good chemical resistance, high thermal stability, and high brittleness) (Table 2.1) [85].

Inorganics can be integrated into organic matrices to increase the RI of materials by a suitable method. As of now, the most frequently employed inorganic materials in the literature reporting high RI organic-inorganic nanocomposites are TiO_2 (n = 2.7 at 500 nm as its rutile form), ZrO_2 (n = 2.2 at 589 nm), ZnO (n = 2.0 at 550 nm), CeO_2 (n = 2.18 at 500 nm) and ZnS (n = 2.4 at 500 nm). These high RI inorganic materials are mostly used as nanoscale building blocks because they can be readily obtained both in the laboratory and commercial purchase. Moreover, some inorganic materials such as ZnO, TiO_2 and CeO_2 are also widely used as UV-shielding pigments in the field of optical research and in the polymer industry [86].

2.1.1. Optical effect of nanocomposites

Optical materials are expected to play a key role in future optoelectronic and information fields. The research on high RI organic-inorganic nanomaterials with excellent mechanical properties and processability is driven by various optical applications, including antireflection coatings, ophthalmic lenses, prisms, optical waveguides, nonlinear optical materials, and adhesives for optical components. Nanocomposites show promise as they can provide the necessary stability and processability. The general principles in the construction of optical nanocomposites involve the intimate mixing of optically functional materials with a processing matrix. By incorporating different inorganic nanoparticles into polymers, many of their interesting optical properties may be enhanced, and the optical films are of great interest as the final form. The major requirement for nanoparticles to be used as fillers for transparent polymers is a small size. Particle diameters below 40 nm are essential to obtain transparent nanocomposites. The reason is the steeply increasing intensity of scattered light with increasing particle diameter as described by Eq. (2.1) (Rayleigh's law):

$$\frac{I}{I_0} = e^{-\left[\frac{3\phi_p x r^3}{4\lambda^4}\left(\frac{n_p}{n_m}-1\right)\right]} \tag{2.1}$$

with intensity I of the transmitted and I_0 of the incident light, radius r of the spherical particles, refractive index n_p of the particles and refractive index n_m of the matrix. λ is the wavelength of the light, Φ_p the volume fraction of the particles and χ the optical path length. A high scattering intensity of visible light is associated with a turbid appearance of the nanocomposite, limiting optical application (Fig. 2.1).

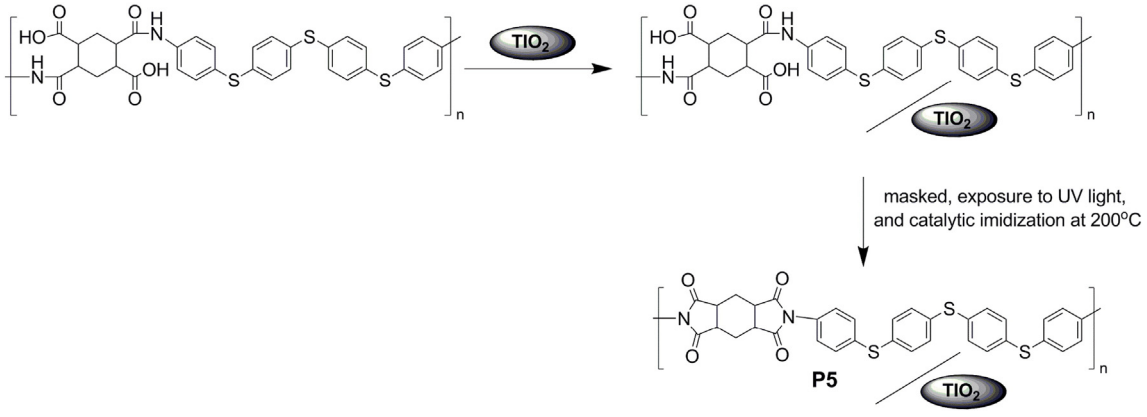

Scheme 2.3. Synthesis of optically transparent TiO_2-PI nanocomposites.

Please cite this article as: C.-L. Tsai, et al., Highly transparent polyimide hybrids for optoelectronic applications, Reactive and Functional Polymers (2016), http://dx.doi.org/10.1016/j.reactfunctpolym.2016.04.021

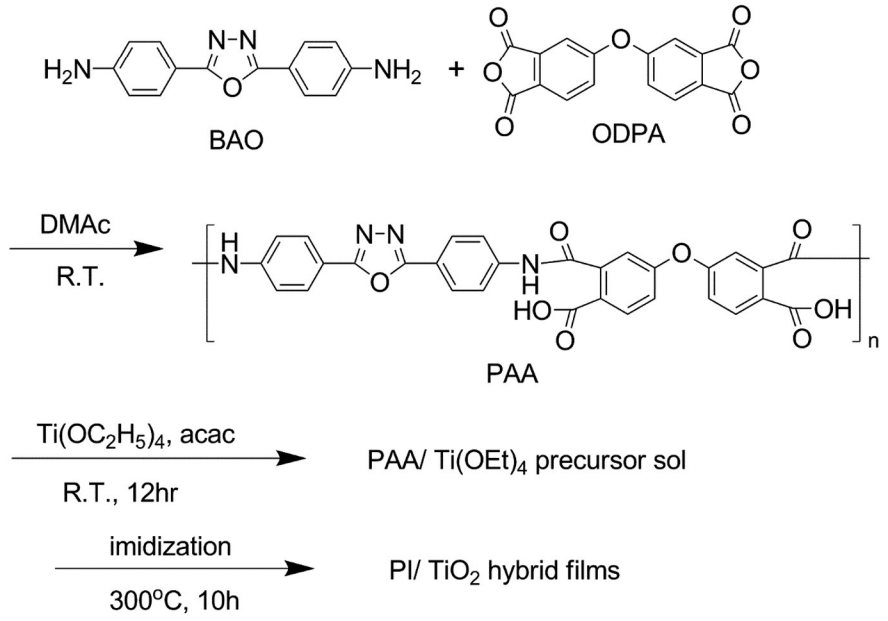

Scheme 2.4. Synthesis of TiO_2-PI nanocomposites by in situ sol-gel process.

However, decreasing the particle size further allows a much more homogeneous distribution of a material and leads to a drastic increase of the polymer/particle interfacial area. The high specific surface area of small nanoparticles may induce their aggregation. Aggregates also lower the homogeneity of particle distribution. A homogenous dispersion of the inorganic filler on the nanoscale is important for many applications, especially when it comes to structure in thin film [87].

2.1.2. High refractive index PIs

It has been well established that the RI values of the conventional polymers (such as poly(methyl methacrylate) (PMMA), polystyrene (PS), polycarbonate (PC)) are often in the range of 1.3–1.6, which are not high enough for co-operative incentive scheme (CIS) applications ($n > 1.8$). Although some special polymer materials, such as wholly aromatic polyamides and aromatic heterocyclic ring backbone polymers ($n = 1.7$–2.0) [88], poly(thiophene) ($n = 2.12$) [89], and aromatic conjugated polymers ($n = 2.7$) [90], can exhibit an RI greater than 1.7, but these polymers usually possess high optical dispersion and large birefringence due to their highly conjugated, aromatic-type, π-electron structures, which, particularly, also tend to be insoluble, poor transparent and deep coloration in the visible region thus restricts their practical application in the field of optics.

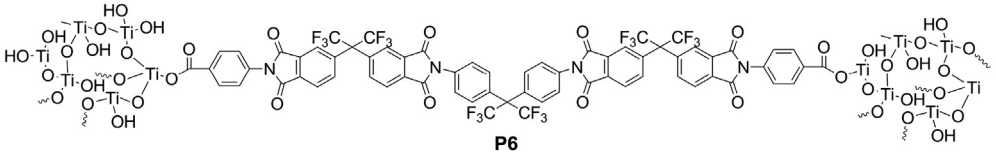

Scheme 2.5. The structure of PI-nanocrystalline titania hybrid material.

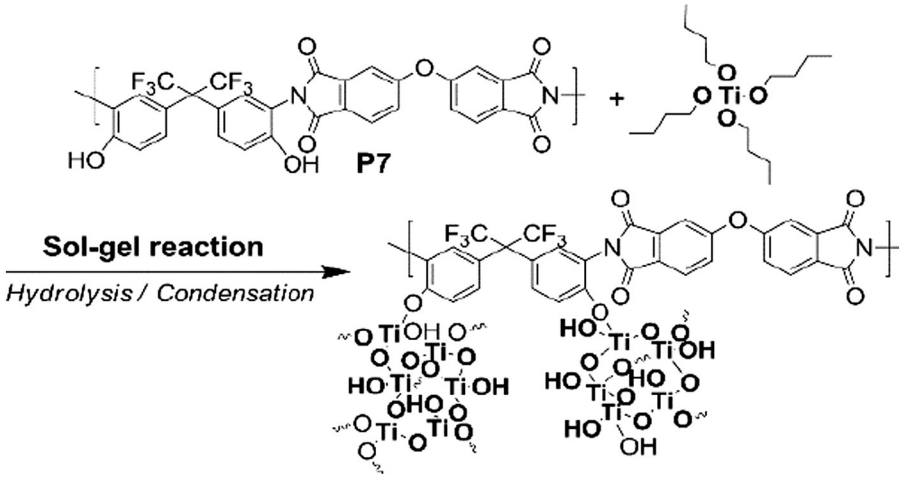

Scheme 2.6. The preparation PI-nanocrystalline titania hybrids from hydroxy-containing PI.

Please cite this article as: C.-L. Tsai, et al., Highly transparent polyimide hybrids for optoelectronic applications, Reactive and Functional Polymers (2016), http://dx.doi.org/10.1016/j.reactfunctpolym.2016.04.021

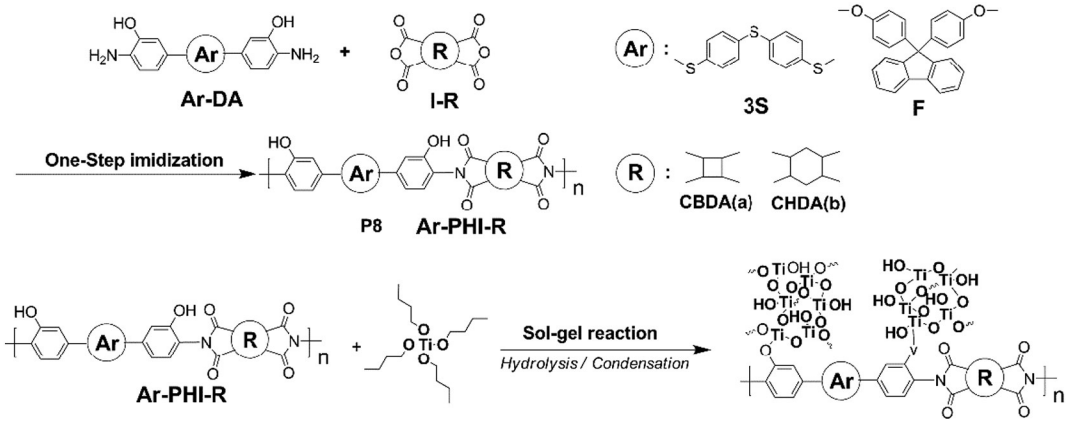

Scheme 2.7. The preparation of PI-nanocrystalline titania hybrids from hydroxy-containing PIs.

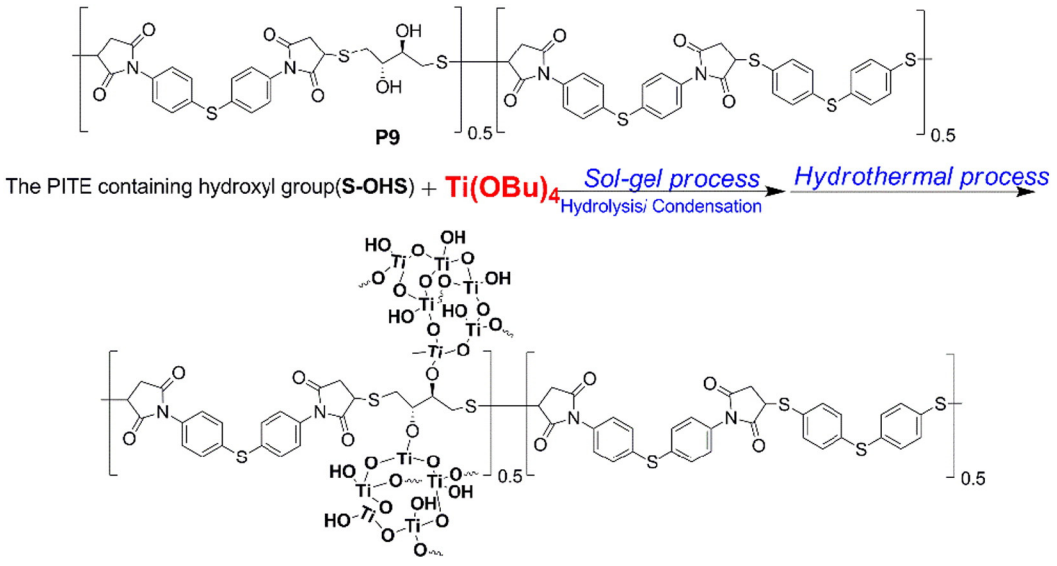

Scheme 2.8. The preparation PITE-nanocrystalline titania hybrids from hydroxy-containing PITE.

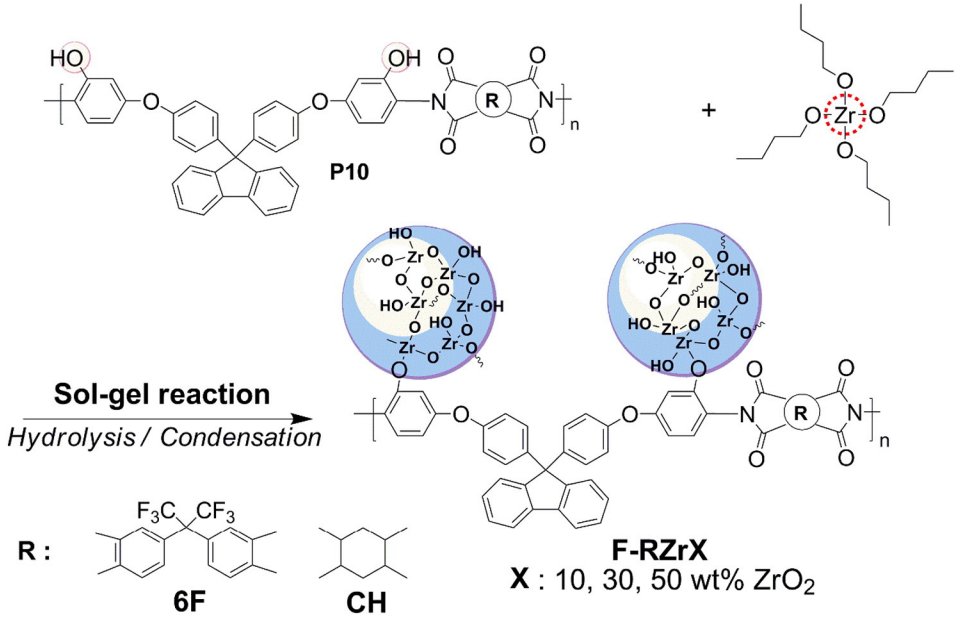

Scheme 2.9. Synthesis and structures of the poly(o-hydroxy-imide)s and PI/zirconia hybrids.

Please cite this article as: C.-L. Tsai, et al., Highly transparent polyimide hybrids for optoelectronic applications, Reactive and Functional Polymers (2016), http://dx.doi.org/10.1016/j.reactfunctpolym.2016.04.021

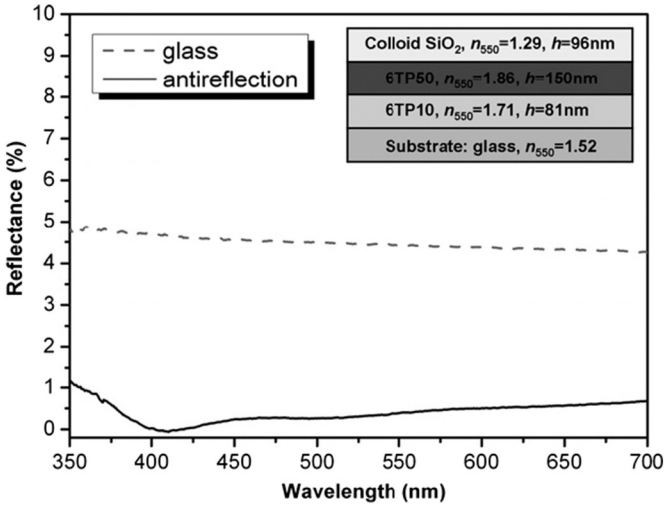

Fig 2.3. Variation of the reflectance with wavelength: BK7 optical glass and the three-layer anti-reflection coating. The insert figure shows the structure of the three-layer anti-reflection coating with **P7**/TiO_2 hybrid films.

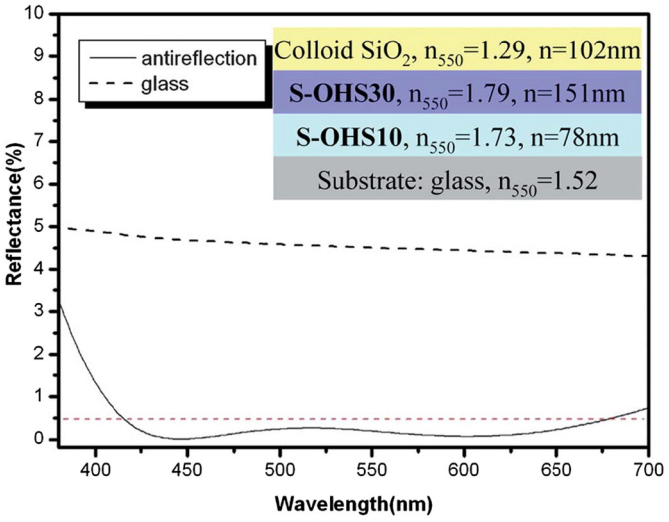

Fig 2.5. Variation of the reflectance with wavelength: BK7 optical glass and the three-layer anti-reflection coating. The insert figure shows the structure of the three-layer anti-reflection coating with **P9**/TiO_2 hybrid films.

Lorentz-Lorenz Eq. (2.2), which described the RI of a material, is related to the molar volume (V_M), polarizability (α) and Avogadro's number (N_A) of the material. The equation also give reliable predictions of the RI of polymers from the group-contribution calculations based on the molar refractions (R_{LL}) of functional groups and the backbone repeating unit of the polymer.

$$R_{LL} = \frac{n^2-1}{n^2+2}\frac{M}{\rho} = \frac{n^2-1}{n^2+2}V \tag{2.2}$$

According to the Lorentz-Lorenz equation, the introduction of substituents with high molar refractions and low molar volumes can efficiently increase the RIs of polymers [91]. It has been well-established that aromatic ring, halogen atoms except fluorine [92], sulfur atoms [93], and metal atoms are effective in increasing the RIs. In particular, the sulfur group might be one of the most promising candidates, which is considered an especially effective way to fabricate high RI polymers with lower dispersion (higher Abbe number).

Recently, many sulfur-containing linear thioether and sulfone, cyclic thiophene, thiadiazole, and thianthrene are the most commonly used moieties for increasing RI of polymers based on conventional poly(methacrylates) (Table 2.2) [93], poly(ethylene glycol) (Table 2.3) [94], polyurethanes (Scheme 2.1) [95], and PIs (Scheme 2.2) [96], which have been developed for advanced integrated optical applications. Among the above mentioned high RI polymers, PIs possess good combined properties, such as excellent thermal stability, high chemical resistance, and high mechanical properties. Quite recently, sulfur-containing new PIs have been prepared for optical application in Ueda's laboratory (**P4**) [89,97]. As summarized in Fig. 2.2, the more the sulfur content, the higher the RI, which can be further proven that sulfur-atom can effectively enhance the RI of the prepared polymers as well as the optical transparency due to its large atomic refraction [79b]. All of them exhibited excellent thermal stability, high RI, good transparency, and low birefringence.

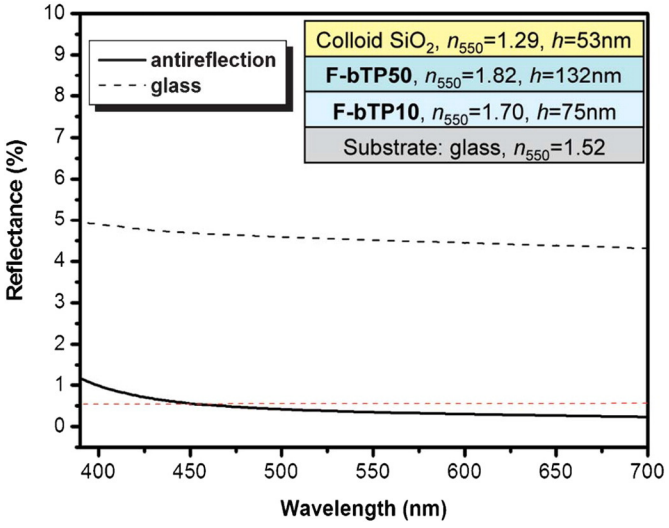

Fig 2.4. Variation of the reflectance with wavelength: BK7 optical glass and the three-layer anti-reflection coating. The insert figure shows the structure of the three-layer anti-reflection coating with **P8**/TiO_2 hybrid films.

2.1.3. PI/titania hybrids

Aromatic PIs prepared from various starting monomers by conventional synthesis routes are promising candidate to incorporate some inorganic nano-clusters, such as titania, into the PI matrix for obtaining hybrid materials. The high glass transition temperature (T_g) of PIs is expected to stabilize the nano-particles by decreasing their mobility, thus could prevent their aggregation to large clusters. However, when the content of titania increases to critical amount, the obtained hybrid films became opaque due to the aggregation of titania into large particles. Therefore, controlling of morphology and domain size of the hybrid materials is important in the preparation of transparent PI/TiO_2 hybrid films [98].

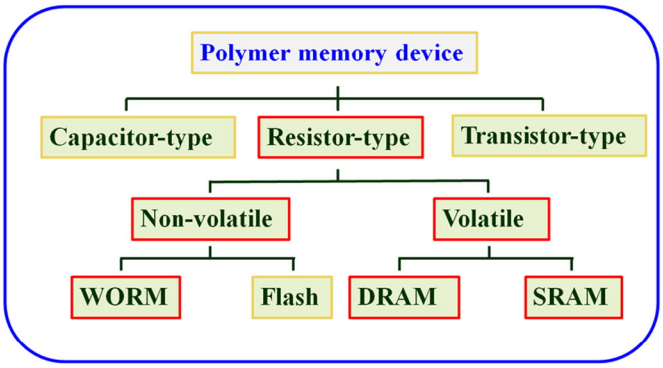

Fig 3.1. Classification of electronic memory devices.

Please cite this article as: C.-L. Tsai, et al., Highly transparent polyimide hybrids for optoelectronic applications, Reactive and Functional Polymers (2016), http://dx.doi.org/10.1016/j.reactfunctpolym.2016.04.021

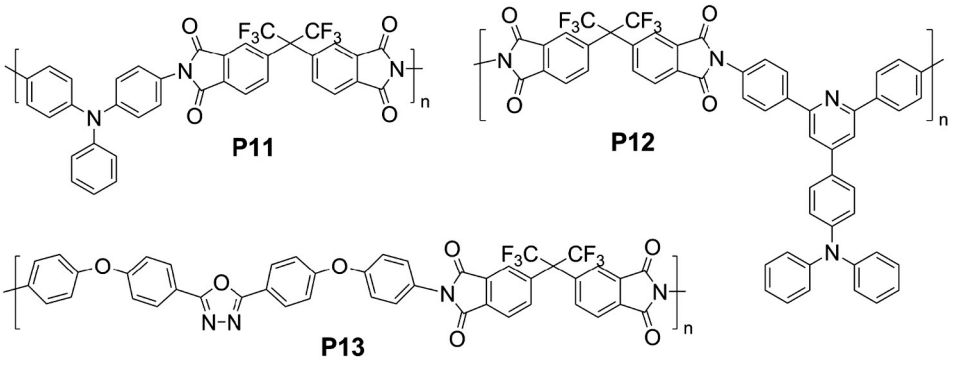

Scheme 3.1. Chemical structure of the PIs **P11**, **P12** and **P13**.

Several PI/TiO_2 hybrid materials with high RI, including the blending method and sol-gel method, have been explored. For the blending method, Ueda lab has developed the optically transparent TiO_2-PI nanocomposites (**P5**) with RI of 1.81 at 633 nm from semi-alicyclic sulfur-containing PAA and silica-modified (provide site isolation) anatase TiO_2 particles with a diameter of 10 nm (n = 2.0 at 589 nm) by the direct blending route (Scheme 2.3) [99].

For the sol-gel method, chemical bonding between the PI and precursor of titania could be produced by using the coupling agents such as aminopropyltrimethoxysilane, and PI/TiO_2 hybrid optical thin films could be prepared via a sol-gel process chelating agent (Scheme 2.4) [98c]. The PI/TiO_2 hybrid thin films also could be successfully fabricated from 2,5-bis(4-aminophenyl)-1,3,4-oxadiazole (BAO) and 4,4′-oxydiphthalic anhydride (ODPA) by an in situ sol-gel process using acetylacetone (acac) as chelating agent. The acac is the most used chelating agent to stabilize the titanium alkoxide because it can reduce the reaction rate through the formation of an acetylacetate complex. However, additional coupling or chelating agent remaining in the hybrid materials might affect important thermal/mechanical/optical properties, and the RIs of such hybrid materials are limited to be around 1.80, which is only slightly higher than recently developed high RI organic polymers. Hence, the development of PI/TiO_2 hybrid optical materials with a higher titania content is necessary. Instead of using poly(amic acid) to prepare their titania hybrid materials, a soluble PI with carboxylic acid end groups (6FDA-6FpDA-COOH) has been synthesized from 4,4′-(hexafluoroisopropylidene)diphthalic anhydride (6FDA), 4,4′-(hexafluoroisopropylidene)dianiline (6FpDA), and 4-aminobenzoic acid (4ABA), as shown in Scheme 2.5. The carboxylic acid end groups can undergo esterification reaction with titanium butoxide ($Ti(OBu)_4$) and provide an organic-inorganic bonding (**P6**), and PI-nanocrystalline titania hybrid materials with high titania content (up to 90 wt%) and RI up to 1.943 could be successfully achieved [100]. However, molecular weight of the polymer is not enough to prepare free-standing PI-TiO_2 hybrid film with higher thickness (20–30 μm) and inorganic content.

Recently, Liou et al. [101] successfully synthesized highly transparent and tunable RI PI-titania and BMI type polyimidothioether (PITE)-titania hybrid optical films from hydroxy-containing organosoluble PIs (**P7**, **P8**) and PITEs (**P9**) with titanium butoxide, respectively, by controlling the organic/inorganic mole ratio (Schemes 2.6, 2.7, 2.8). The hybrid thin films had good surface planarity, high thermal stability, tunable refractive indices, and high optical transparency in the visible range. Moreover, the thick titania hybrid films could also be achieved even with a relatively high titania content. The RI (up to 1.92) and titania content (50 wt.%) are the highest among the highly optical transparent polymer–titania hybrid thick films (15–20 μm thick). The three-layer antireflective coating based on the hybrid films exhibited a reflectance of less than 1.0% in the visible range. It suggests potential optical applications of the novel PI–titania hybrid optical films.

2.1.4. PI/zirconia hybrids

Recently, polymer-inorganic hybrid materials have attracted a great deal of attentions owing to the outstanding combinations of mechanical,

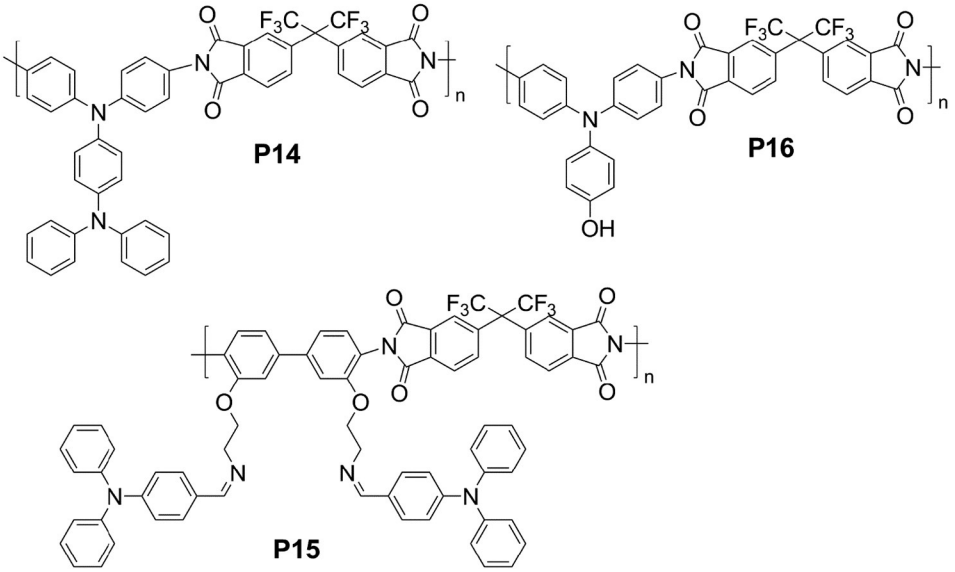

Scheme 3.2. Chemical structure of the PIs **P14**, **P15** and **P16**.

Please cite this article as: C.-L. Tsai, et al., Highly transparent polyimide hybrids for optoelectronic applications, Reactive and Functional Polymers (2016), http://dx.doi.org/10.1016/j.reactfunctpolym.2016.04.021

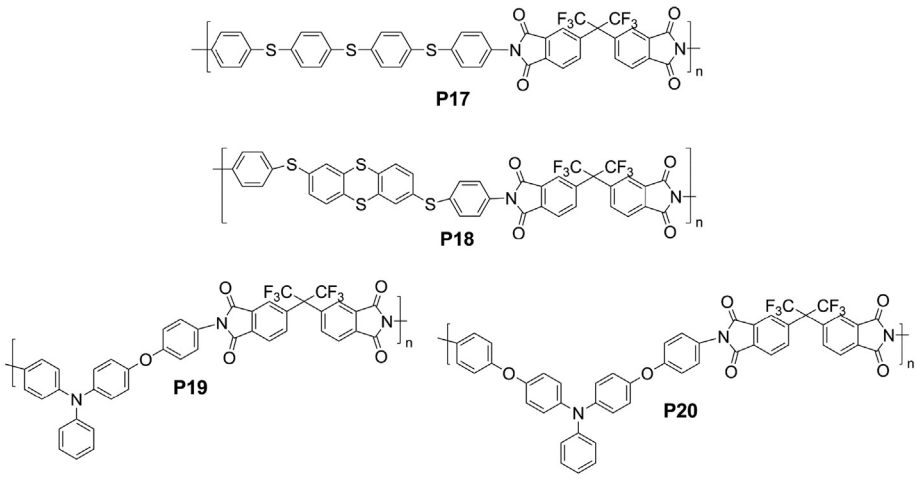

Scheme 3.3. Chemical structure of the PIs **P17**, **P18**, **P19** and **P20**.

thermal, magnetic, optical, electronic, and optoelectronic properties when compared with individual polymer or inorganic components [102]. Chemical bonding approaches based on in-situ sol-gel reaction made it possible to overcome the agglomeration phenomenon of inorganic nanoparticles by manipulating the organic/inorganic interactions at various molecular and nanometer length scales, and the PI/TiO_2 hybrids with high RI could be achieved by increasing TiO_2 content, which is reported Liou's lab [101]. However, the optical transparency of the obtained PI/TiO_2 hybrid films reduced dramatically at wavelength around 400 nm due to the low band gap of TiO_2 (3.2 eV), resulting in pale yellow color of the hybrid films. Besides, Abbe number of the PI/TiO_2 hybrid films also decreased with increasing TiO_2 content. Thus, by choosing species of inorganic materials in the hybrid system for enhancing the RI without sacrificing Abbe number and optical transparency in visible light region is an important issue.

Therefore, Liou reported highly transparent and flexible PI/Zirconia (ZrO_2) nanocomposite optical films with tunable RI and Abbe number (Scheme 2.9) [103]. Because ZrO_2 has excellent combination of optical properties, such as high RI, Abbe number, and transparency on a broad spectral range due to the large band gap of ZrO_2 in the range 5.0–5.85 eV [104]. Therefore, a facile in-situ sol-gel approach for obtaining optically transparent PI/ZrO_2 hybrids was used, and the pendent hydroxyl groups in PIs (**P10**) prepared from the fluorene-containing diamine with commercial dianhydrides 6FDA and CHDA, respectively, could provide the organic-inorganic bonding sites with zirconium butoxide ($Zr(OBu)_4$) to obtain PI/ZrO_2 hybrid films with different ZrO_2 contents for advanced optical applications. Moreover, these PI/ZrO_2 hybrid films also revealed much higher optical transparency than the corresponding PI/TiO_2 system due to the large band gap of ZrO_2 resulting in much shorter absorption wavelength edge of ZrO_2 (230 nm) than that of TiO_2 (400 nm). In addition, the 100 wt% ZrO_2 thin film also exhibited superior optical transparency (96%) at 450 nm of wavelength than 100 wt% TiO_2 thin film (88%). Besides, the RI and Abbe number of the resulting PI/ZrO_2 hybrid system are tunable and up to 1.804 and 32.18, respectively, by increasing zirconia content. These results demonstrate that PI/ZrO_2 hybrid system is an excellent alternative for high-performance optical materials.

2.2. Multilayer antireflection coatings

Optical materials are expected to play a key role in the optical, optoelectronic, and information fields. The researches on high RI organic-inorganic hybrid materials with excellent mechanical properties and processability is driven by various optical applications, including antireflection coatings, ophthalmic lenses, prisms, optical waveguides, nonlinear optical materials, and adhesives for optical components, etc.

Antireflective (AR) coatings were applied to diminish the reflection loss at the surface of an optical component and obtain a clear view through the glazing by increasing light transmittance and avoiding negative effects on the visual observation, like double image, reflection of light sources, etc. [105]. The high RI hybrid materials may play a more important role in the design of gradient-index AR coatings for higher RI substrates or device surfaces due to their tunable RI. Recently, Liou et al. [101] prepared the three-layer *anti*-reflective coating on the BK7 glass substrate (Figs. 2.3, 2.4, 2.5). The BK7 optical glass has a RI ($n = 1.518$) higher than air ($n = 1.0$) and leads to an average reflectance of about 5% in the visible range. The reflectance could be reduced significantly via a three-layer anti-reflection coating consisting of polymethyl silsesquioxane (PMSSQ) and two PI hybrid films with different TiO_2 content as the first, second, and third layers, respectively. In order to

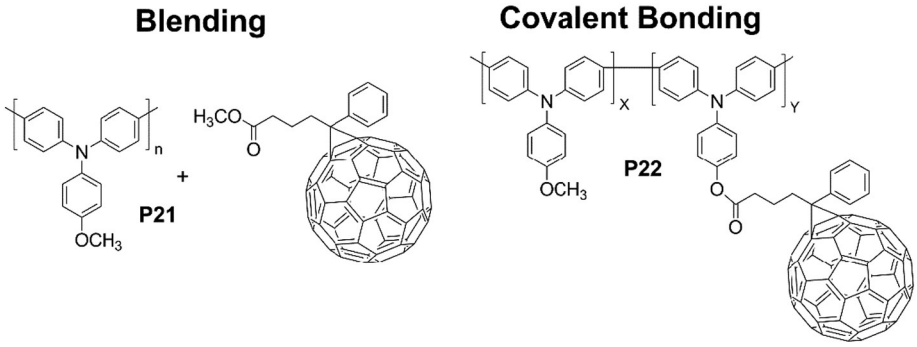

Scheme 3.4. Polymer hybrids with PCBM by blending and covalent bonding.

Please cite this article as: C.-L. Tsai, et al., Highly transparent polyimide hybrids for optoelectronic applications, Reactive and Functional Polymers (2016), http://dx.doi.org/10.1016/j.reactfunctpolym.2016.04.021

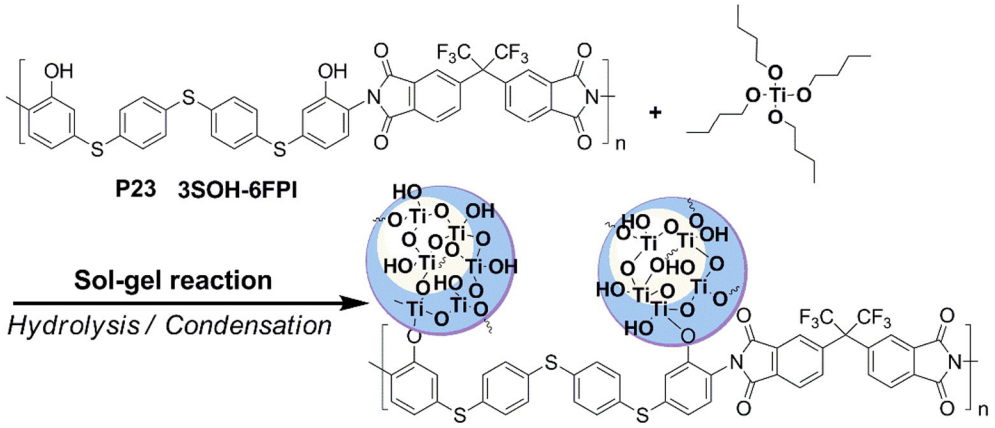

Scheme 3.5. PI/TiO_2 hybrids with covalent bonding by in situ sol–gel reaction.

reduce reflection through adjusting the phase of light, the optical thickness (physical thickness × refractive index) is designed to be 0.25 λ_0, 0.5 λ_0, and 0.25 λ_0 ($\lambda_0 = 550$ nm) for the three-layer structure. By applying the three-layer anti-reflection coating, an average reflectance of less than 0.5% in the visible range can be obtained, which is significantly smaller than that of BK7 with 5%. The result suggests the potential application of the prepared PI/TiO_2 hybrid films in optical devices.

3. Highly transparent PI hybrids for electrical applications

3.1. Resistive type switching memory devices

Devices incorporating switchable resistive materials are generically classified as resistor-type memory, or resistive random access memory (RRAM). Based on retention time after removing power, electronic memories can be divided into two primary classifications: volatile and non-volatile memories. Volatile type could erase the stored data as soon as the system is turned off, and the constant power supply is necessary for keeping information stored. However, non-volatile type can retain the stored information even when the electrical power supply has been removed. The non-volatile type can be further divided into sub-categories, as shown in Fig. 3.1, with the write-once-read-many times (WORM) memory and non-volatile rewritable (flash) memory. The difference between these two is that WORM type can keep data permanently and not allow erasing the data (once it has written as CD-R, DVD ± R). Flash type memory stored state can be electrically reprogrammed and it has the ability to write, read, erase and retain the stored data, and it have been used in many portable electronic systems, such as mobile computer, PDA, cell-phone, and digital camera etc. On the contrary, volatile type includes the dynamic random access memory (DRAM) and the static random access memory (SRAM). DRAM exhibits ability to write, read, erase and refresh the electric states; and SRAM possess longer storage time after removing the electrical field. Nowadays, DRAM is used commonly as memory devices in computer.

Resistive switching behavior has been primarily studied in amorphous silicon-based materials for the past 30 years. It was found that the digital data could be stored by applying or discharging electrical charges through a simple device configuration consisting of two electrode layers sandwiching the storage medium. As compared to the traditional inorganic semiconductor-based memories, polymeric memory devices are extensively attractive because of the advantages of low cost, solution processability, miniaturized dimensions and three-dimensional stacking capability, and structural flexibility through molecular design and chemical synthesis. The recently investigated polymeric systems exhibit memory switching characteristics, including

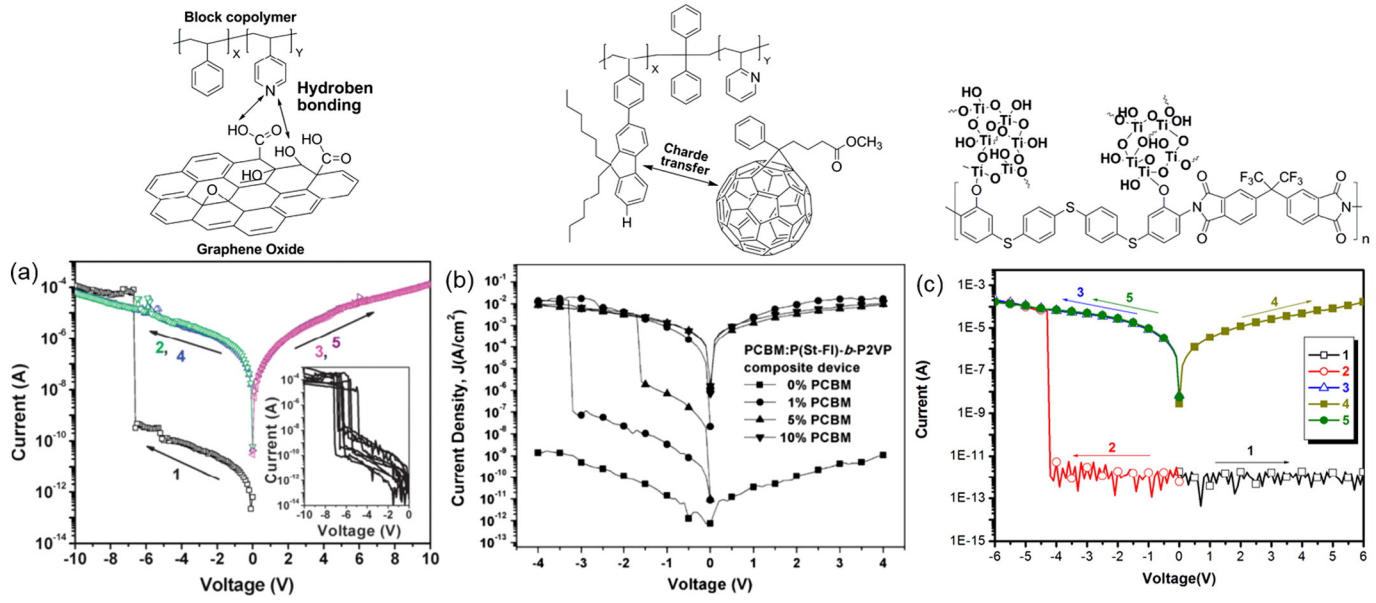

Fig 3.2. (a) *I–V* characteristics of 7 wt% GO/Block copolymer composite device. The inset shows the switching behavior in different memory cells. (b) Current density vs. voltage plots for ITO/PCBM:P(St-Fl)-*b*-P2VP/Al composites devices. (c) Current-voltage (*I–V*) characteristics of the ITO/hybrid material (3STP-10)/Al memory devices.

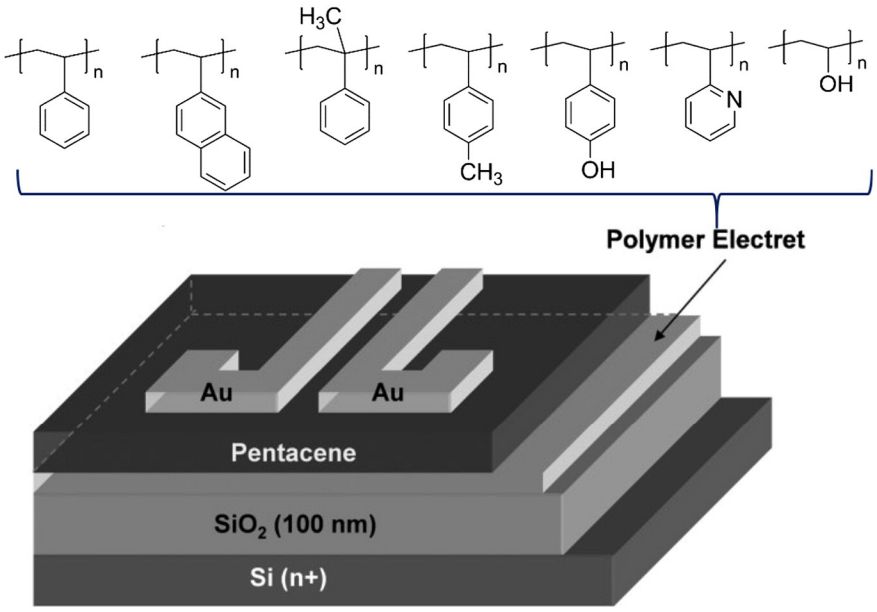

Fig. 3.3. Various styrenic polymer were used in this polymer electrets memory device.

conjugated polymers, functional PIs, polymers with specific pendant chromophores, and polymer nanocomposites (metal nanoparticle and fullerene embedded), are promising candidates for future molecular-scale memory applications. The electrical switching phenomena in polymers and the corresponding polymer electronic memories as an emerging area in organic electronics have been reviewed by Kang et al. [106].

3.1.1. PI-based memory devices

PIs are promising candidates for memory device applications because of their excellent physical and chemical properties in addition to the electrical switching behavior [107]. Functional PIs containing both electron donor and acceptor moieties within a repeating unit contribute to electronic transition between the ground and excited states, which could be manipulated by the induced charge transfer (CT) from donor (D) to acceptor (A) under applied electric fields. Among the reported functional PIs, the triphenylamine (TPA)-based PIs reported by Liou et al. [108] have attracted significant attentions. For example, the memory device derived from TPA-containing PI (**P11**) [109] exhibited dynamic random access memory (DRAM) behavior, whereas a device based on **P12** [110] showed the improved DRAM performance as reported by Kang and coworkers (Scheme 3.1), and an oxadiazole-containing PI (**P13**) [111] was found to reveal a static random access memory (SRAM) behavior. Meanwhile, Ree and Liou et al. [112] also proposed a series of TPA-based PIs for memory characteristics. They found that **P14** (two connected TPA units) (Scheme 3.2) showed digital WORM and volatile DRAM memory characteristics depending on film thickness. Moreover, a flash type memory of **P15** [113] bearing two pendant TPA groups and a unipolar WORM memory of **P16** [114] having an attached hydroxyl group on TPA were also reported recently. Ueda and Chen [115] prepared sulfur-containing PIs (**P17**, **P18**) (Scheme 3.3), and demonstrated that the relatively high dipole moments of the sulfur-containing PIs provided a stable CT complex for the flash memory device with nonvolatile memory characteristics and low turn-on threshold voltages. They further synthesized two functional PIs (**P19** and **P20**) consisting of electron-donating TPA with single and double isolated ether linkage, respectively, and electron-accepting phthalimide moieties. The memory devices with the configuration of **P19**/Al or ITO/**P20** exhibited distinct volatile memory characteristics of DRAM and SRAM, respectively. The result provides the strategy for the design of functional PIs in advanced memory device applications.

3.1.2. PI/TiO_2-based memory devices

Recently, the hybrid composites were extensively prepared for memory device applications. CT complex formation could be further enhanced by the introduction of supplementary components such as

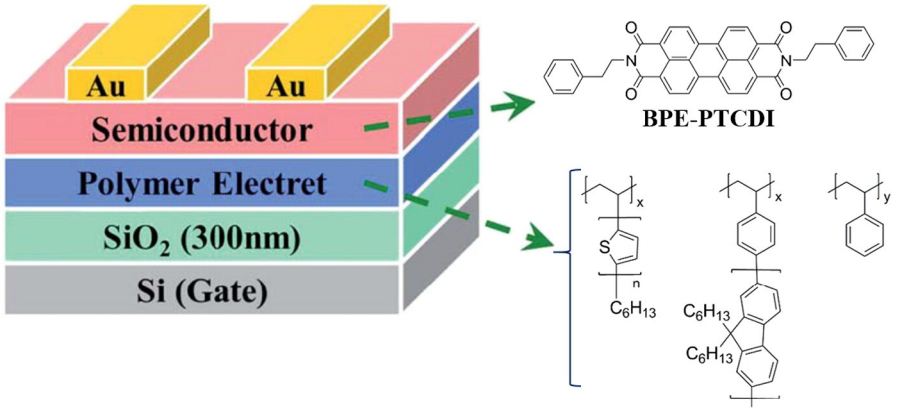

Fig. 3.4. Schematic structure of the BPE-PTCDI thin film based OFET memory device.

Please cite this article as: C.-L. Tsai, et al., Highly transparent polyimide hybrids for optoelectronic applications, Reactive and Functional Polymers (2016), http://dx.doi.org/10.1016/j.reactfunctpolym.2016.04.021

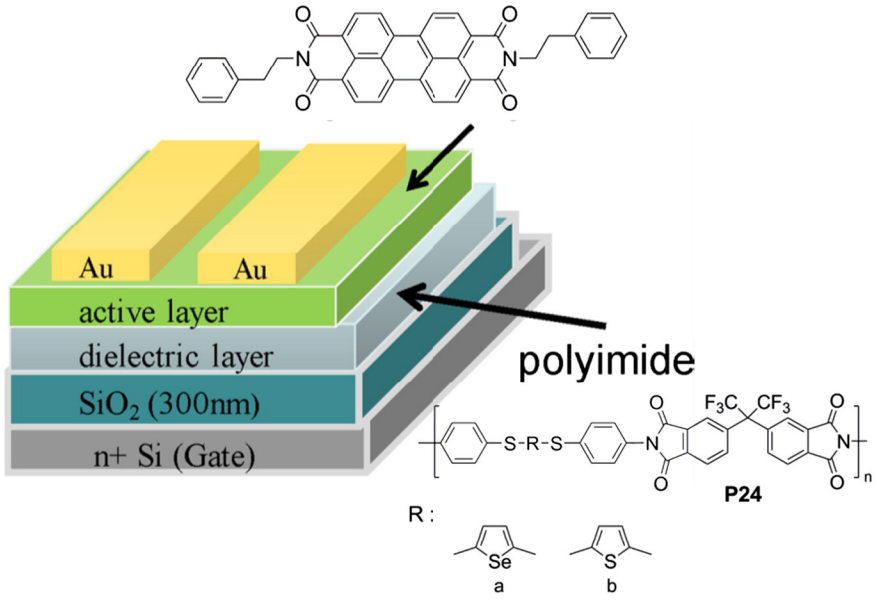

Fig 3.5. The structures of **P24a** and **P24b**.

organic molecules or metallic particles serving as electron donors or electron acceptors in polymer matrix [116]. As compared to the polymer memory devices with organic molecules or metallic particles, relatively few studies have been conducted on the polymer memory devices containing semiconducting particles [117].

Very recently, memory devices were fabricated by blending PCBM, as the acceptor, with donor-containing poly(4-methoxytriphenylamine) (**P21**) (Scheme 3.4) [118] in Liou's group. The memory devices with the configuration of ITO/PCBM:**P21**/Al exhibited both DRAM and WORM properties controlled by the concentration of PCBM. The strong interaction between PCBM and TPA could be a result of well-dispersed PCBM clusters within PCBM:**P21** hybrid films. The obtained hybrid films revealed bistable WORM behavior at higher concentration up to 10 wt% PCBM. However, when compared with the high ON/OFF contrast ratio of 5 wt% PCBM:**P21**, the memory device using 10 wt% PCBM:**P21** showed much lower contrast ratio. While, by introducing 10 wt% PCBM into **P22** via covalent bonding [119], the polymer hybrids with covalent bonding between PCBM and polymer chain could improve the dispersion of PCBM in polymer matrix, resulting in WORM memory device with lower switching-ON voltage and much higher ON/OFF ratio than that of corresponding blending hybrids. Besides, the memory behavior remained very well under the heating condition up to 100 °C. This is crucial for maintaining device stability in computer applications even other components produce heat.

Furthermore, the PI **P23**/TiO_2 hybrids with covalent bonding by in situ sol-gel reaction (Scheme 3.5) [120] were also used to investigate the feasibility for memory application. Because of the low LUMO energy level (4.2 eV) [121], TiO_2 could serve as an electron acceptor in hybrid system to facilitate and stabilize CT complex formation for increasing retention time of memory characteristic in device application. Comparing with conducting supplementary components such as PCBM, CNT, graphene, and metallic particles [118,122], the introduction of TiO_2 could also prevent the detriment of decreasing ON/OFF ratio at high TiO_2 content, resulting in the lower conductivity in the OFF state (Fig. 3.2) [120b].

These PI/TiO_2 hybrid films with different TiO_2 concentration from 0 wt% to 50 wt% showed very small domain size of TiO_2 around 3–5 nm, and the obtained memory properties could be tuneable from DRAM, SRAM, to WROM with high ON/OFF current ratio by adjusting different hybrid amount of TiO_2 [123]. Furthermore, the *I—V*

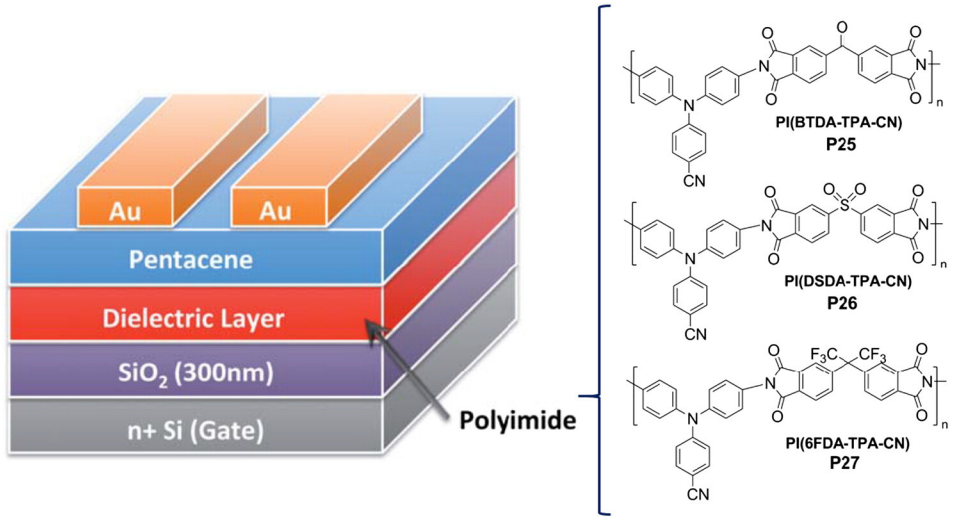

Fig 3.6. The structures of **P25–P27.**

Please cite this article as: C.-L. Tsai, et al., Highly transparent polyimide hybrids for optoelectronic applications, Reactive and Functional Polymers (2016), http://dx.doi.org/10.1016/j.reactfunctpolym.2016.04.021

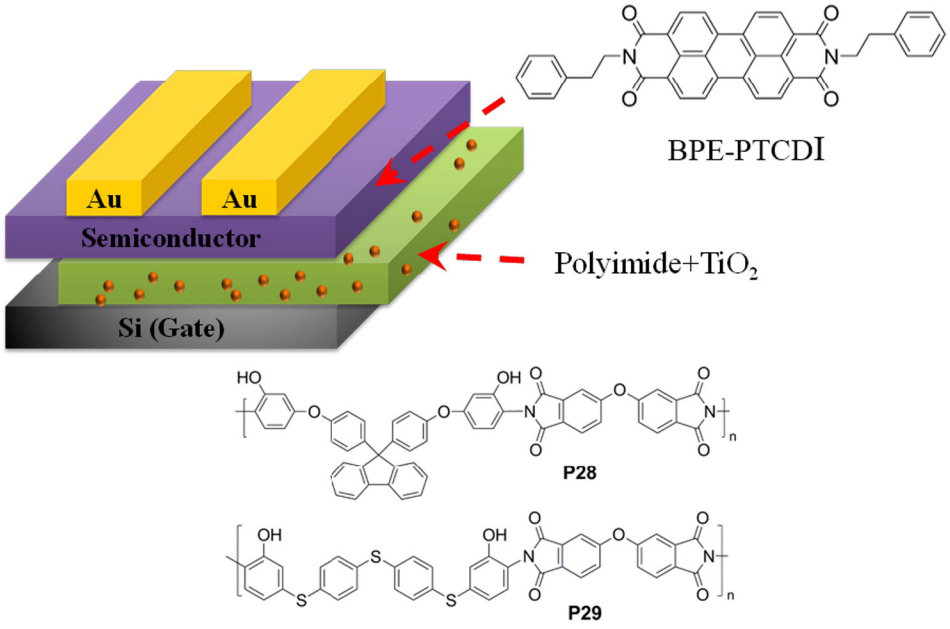

Fig. 3.7. Schematic structure of the BPE-PTCDI thin film based OFET memory device with PIs **P28** and **P29**.

characteristic indicates that the memory devices based on amorphous TiO_2 hybrids have shorter retention time at the ON state comparing to crystalline TiO_2 hybrid system [124].

3.2. Transistor memory device

Organic field effect transistor (OFET) type memories have attracted a great deal of attentions due to easily integrated structure, non-destructive reading, and multiple-bit storage in a single transistor [125]. The device configuration for conventional transistors consisted an additional polymer dielectric layer (refer to as polymer electret) between a semiconductor layer and gate contact. Polymer electrets are dielectric materials which exhibit a long-term charge storing ability or electrostatic polarization, including the chargeable polymer electret [126], organic ferroelectric oriented-dipole dielectric materials [127], and nanoparticles (NPs) embedded or nanostructured gate dielectrics [128]. Kim and his coworkers described that the charge trapping ability of poly(α-methyl styrene) electret could induce memory characteristics of the pentacene-based OFET device [126b], and also demonstrated that the hydrophilicity and dielectric polarity of polymer electrets significantly affected the device performance (Fig. 3.3) [129]. Recently, the nonvolatile flash memory characteristics of *N*,*N*′-bis(2-phenylethyl)-perylene-3,4:9,10-tetracarboxylic diimide (BPE-PTCDI) based transistors containing different pendent conjugation length were also reported (Fig. 3.4) [130].

Recently, Chen's and Liou's groups reported that the intensity of charge transfer in D-A PI electrets, **P24a** and **P24b**, which could significantly affect the memory window of n-type BPE-PTCDI-based OFET memory devices (Fig. 3.5) [131]. Furthermore, the OFET devices derived from TPA-based PI electrets with higher dielectric constant (k) were also fabricated and demonstrated the enhanced capability for storing the charges (**P25**–**P27**) (Fig. 3.6) [132].

In fact, one of the major challenges in the development of OFETs is that rather high voltage needs to operate devices when using organic gate dielectrics, making these devices impractical for low-priced applications. The key to low-voltage application resides in the reduction of the threshold voltage and the inverse sub-threshold slope. Both parameters are basically controlled by the gate insulator. Therefore, using high-k hybrid electrets might be a promising approach to conduct the devices at lower voltage. Manipulation of the dielectric layer could be accomplished by using inorganic/organic hybrid dielectric materials because of their robust insulating property and ease of processing. By introducing PI into the hybrid materials not only could obtain tough and good quality electrets films via solution-casting but also preserve the advantages and characteristics of high permittivity of the inorganic inclusions, and high breakdown strength, flexibility, high mechanical strength of PI in this hybrid materials. Lee et al. [133] reported that the performance OFET device could be improved significantly when a high-k PI hybrid was used as a gate dielectric by blending different concentration of polyester-modified TiO_2 nanoparticles into a PI matrix. However, one of the critical drawbacks for these hybrid films is high leakage current that limits their use in OFETs. Therefore, sol-gel technique might be a good approach for the preparation of TiO_2 particles to suppress the leakage current of devices because the obtained TiO_2 particles have nano-scale domain size, narrow particle distribution, and excellent dispersion over the polymer matrix. Liou and Chen groups reported that the BPE-PTCDI OFET memory device based on the **P28** electret with conjugated fluorene moiety exhibited the larger memory

Table 3.1
Examples for AgNWs transparent heaters.

Substrate	R_s (Ω/sq)	$T_{550\ nm}$ (%)	FoM	Max temp./applying voltage	Note	Ref.
PET	10	75	120	47 °C/4V	Spray coating	[136a]
Glass	27	80	60	225 °C/15V	Hybrid with graphene oxide Filter transferring	[135a]
Polyacrylate	25	85	90	160 °C/11V	Heat-resistance polyacrylate Transferring coating	[135b]
PEDOT:PSS	4	70	240	110 °C/6V	Rod casting	[136b]

Please cite this article as: C.-L. Tsai, et al., Highly transparent polyimide hybrids for optoelectronic applications, Reactive and Functional Polymers (2016), http://dx.doi.org/10.1016/j.reactfunctpolym.2016.04.021

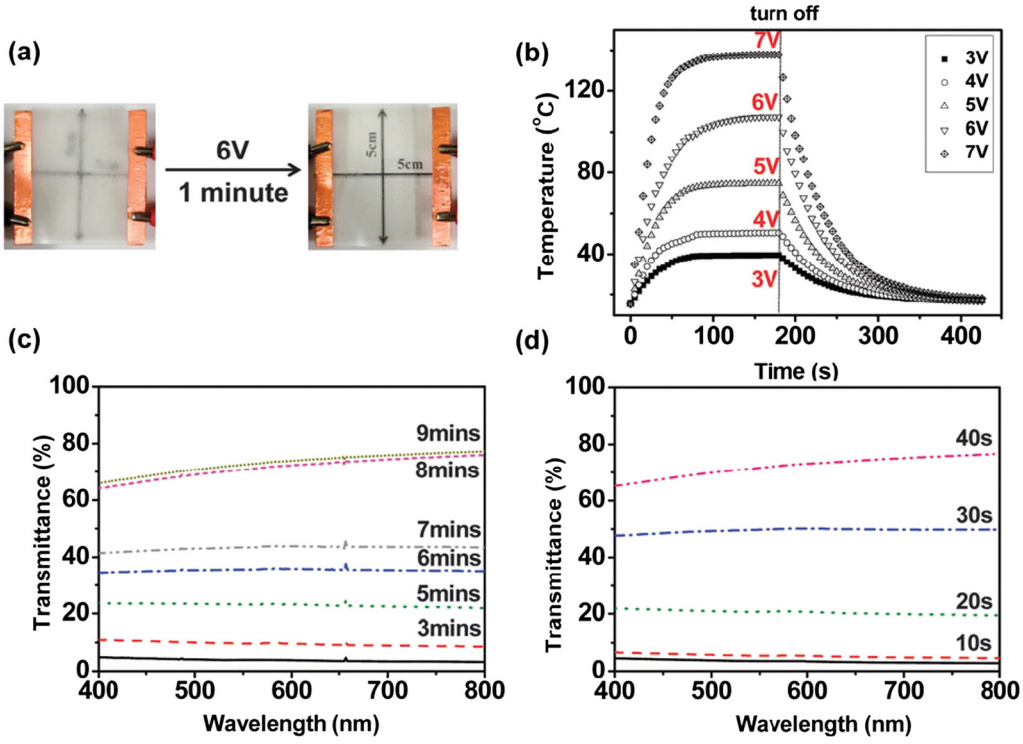

Fig 3.8. (a) The defogging device fabricated from PI/AgNWs hybrids was put in a refrigerator and then subjected to an applied potential of 6 V, the water on the surface was removed after only one minute. (b) The temperature plotted against time at various applied potentials. (c) UV–vis spectra for the defogging device without any applied potential. (d) UV–vis spectra for the defogging device with an applied potential of 6 V.

window compared to **P29** (Fig. 3.7) [134]. In addition, BPE-PTCDI-based OFET nonvolatile memory devices using PI/TiO_2 hybrids with higher dielectric constant as electrets revealed not only reducing the operating voltage but also increasing memory window, ON/OFF ratio, and the stability at ON or OFF states over 10^4 s. Thus, the novel PI/TiO_2 hybrids with high dielectric constant as electrets have potential for high performance nonvolatile OFET memory devices.

3.3. Defogging device based on transparent PI/AgNW electrode heater

Transparent electrodes based on AgNWs network also could be used as heater according to Joule's law shown in Eq. (3.1), where Q_g is abbreviation of generated heat, V is the applied voltage, t is the heating time, and R is the resistance of the film heater over which the voltage is applied. The heat generated by electrode is estimated in fixed sheet resistance and applying voltages. Therefore, AgNWs network also selected as a candidate for applying in defogging device of windshield. In order to determine saturation temperature of heater, the estimation of heat dissipation (Q_d) is an important factor needed to be concerned. Q_d involves thermal conduction (through the substrate and air), radiation, and convection. For most of studies in PI/AgNWs hybrid heaters, thermal conduction is neglected due to the thermal insulator properties of hybrid film (or substrate). Regarding heat radiation, studies had given two different estimations of its contribution to the heat dissipation of heaters. Some researchers neglected it by considering the low temperature of heaters (<150 °C) [135], while others deemed as an important contribution on it [136]. According to Stefan-Boltzmann law, the radiation dissipation (Q_{rd}) is expressed as Eq. (3.2), where T_0 is surrounding temperature, T is heater's temperature, A is the surface area, ε is the surface emissivity, s is the Stefan-Boltzmann constant (5.67×10^{-8} W m^{-2} K^{-4}), and h_R is the temperature-related radiation heat transfer coefficient. The surface emissivity of polymer substrate has a value close to 0.9 h_R varies from 5.4 to 9.8 W m^{-2} K^{-1} when the temperature increases from 25 to 150 °C. In the other hand, the surface emissivity of silver is about 0.2 h_R changing from 1.2 to 2.2 W m^{-2} K^{-1} in the same temperature variation [136b]. Thus, the total heat transfer coefficient h_T ($h_T = h_C + h_R$) could be substituted into Eq. (3.1) and heat capacity equation. The derivative equation is shown in Eq. (3.3). After solving the Eq. (3.3), the saturated temperature of the AgNWs heater could be estimated (Eq. (3.4)) which showed much more precise than Eq. (3.1). Similarly, the cooling equation

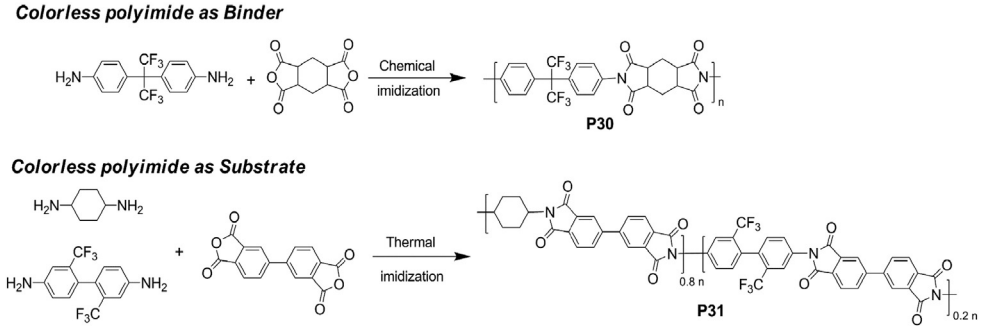

Scheme 3.6. The synthetic scheme for the colorless polyimides.

Please cite this article as: C.-L. Tsai, et al., Highly transparent polyimide hybrids for optoelectronic applications, Reactive and Functional Polymers (2016), http://dx.doi.org/10.1016/j.reactfunctpolym.2016.04.021

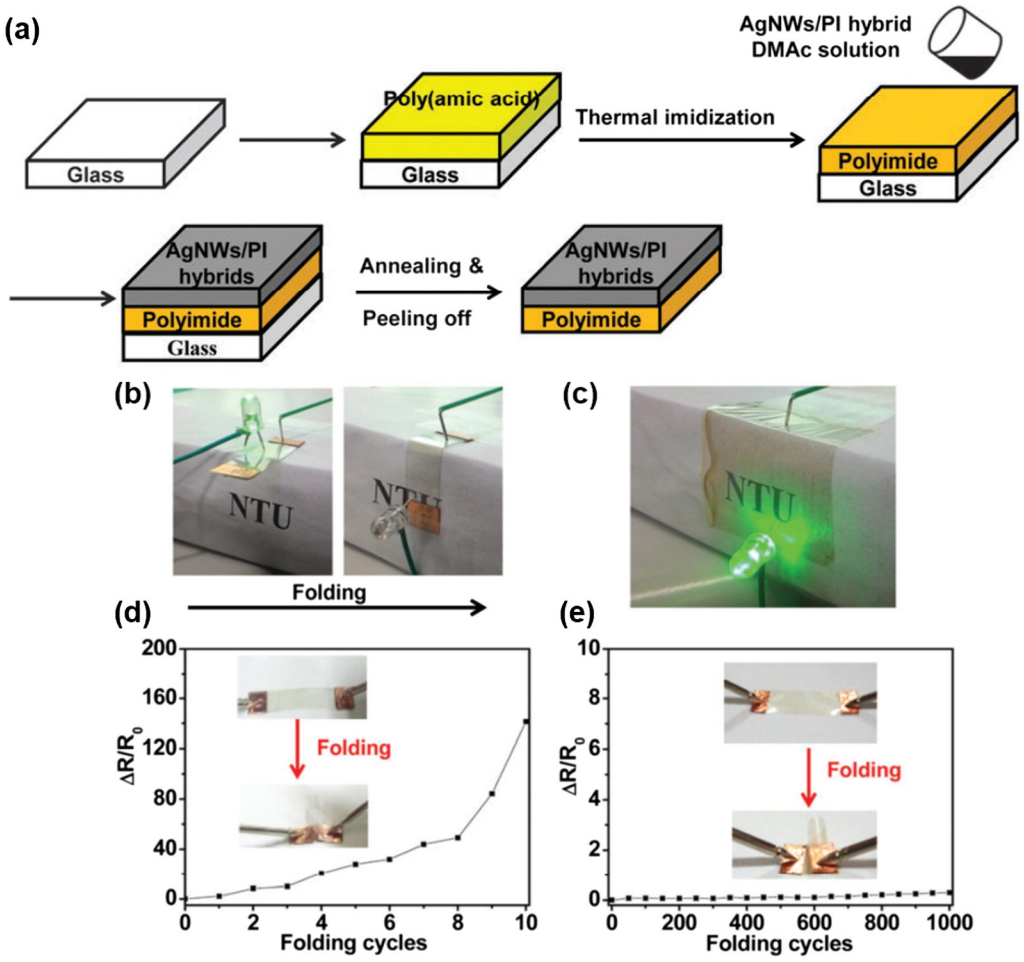

Fig 3.9. (a) The scheme of the procedure for the transparent PI/AgNWs hybrid electrodes. Two kinds of PI were used as both the binder and substrate. (b) The ITO coated PEN lost conductivity immediately after folding, thus the LED lamps no longer worked. (c) The PI/AgNWs hybrid electrode connected to a LED array. The LED lamps kept working even under continuous folding conditions. (d) The change in resistance after folding for the ITO coated PEN electrodes. The Y-axis represents the change in resistance divided by the original resistance. (d) The change of resistance after 1000 folding cycles for the PI/AgNWs hybrid electrodes.

also derived as shown in Eqs. (3.5) and (3.6) that only consider heat dissipation. Another factor (such as size effect of AgNWs with different temperature) has been added into equations by some groups to achieve more precise temperature value. However, the effect is neglected for most of researches due to the lack of influence.

The examples of AgNWs transparent heater are summarized in Table 3.1. Most of AgNWs hybrid heaters based on PET substrate are limited due to the lack of thermal stability. Thus, maximum saturated temperature of heater only reached to about 110 °C. While, AgNWs-glass heater could stand up to the temperature up to 225 °C, implying high potential of the AgNWs heaters [135a]. Thus, higher thermal-resistant polymers such as high performance polyimides are introduced in hybrid system for enduring heat generated from AgNWs [135b]. However, the maximum temperatures, organic-soluble behavior, and deep coloration of these polymers still resulted in insufficient to endure high temperature or post film-processing for practical application.

$$Q_g = \frac{V^2 t}{R_s} \tag{3.1}$$

$$Q_{rd} = \varepsilon s A\left(T^4 - {T_0}^4\right) = \varepsilon s A\left(T^2 + {T_0}^2\right)(T + T_0)(T - T_0) = A h_R (T - T_0) \tag{3.2}$$

$$CdT = \frac{V^2}{R}dt - hA(T - T_0)dt \tag{3.3}$$

$$T = T_0 + \frac{V^2}{RhA}\left(1 - e^{-\frac{hA}{C}t}\right) \tag{3.4}$$

$$CdT = -hA(T - T_0)dt \tag{3.5}$$

$$T = T_0 + (T_{off} - T_0)e^{-\frac{hA}{C}\left(t - t_{off}\right)} \tag{3.6}$$

Recently, Liou et al. reported the defogging devices fabricated by the PI/AgNWs hybrid electrodes which defog effectively within one minute at applied potential of 6 V [137]. The higher the applied potential on the device, the higher temperature could be reached. As the applied potential was increased to 7 V, temperature higher than 130 °C could be obtained (Fig. 3.8). Therefore, the thermal stability of both the substrates and binders should be good enough to withstand such high temperatures, and that will not be an issue when using PI as substrates and binders. For the application of windshields in automobiles, the occurrence probability of an accident may be reduced by removing condensed water on the windshield more effectively. Moreover, this approach can also replace the traditional defogger on a vehicle's rear windshield, which consists of a series of parallel linear resistive conductors. Without the parallel linear resistive conductors on the back glass, it would be more pleasing to the eyes.

Please cite this article as: C.-L. Tsai, et al., Highly transparent polyimide hybrids for optoelectronic applications, Reactive and Functional Polymers (2016), http://dx.doi.org/10.1016/j.reactfunctpolym.2016.04.021

3.4. Electrochromic devices based on PI/AgNWs electrode

With the technology advancing, all kinds of electronic products developed rapidly. Especially for monitor devices, large requirements and phenomenal development speed revealed the importance of transparent electrode. Although the family of metallic oxides such as indium tin oxide (ITO) has occupied most of the market due to the excellent properties in electrical and optical behavior, brittle property and high cost are the crucial problems need to face with [138]. Therefore, the novel replacements have attracted great attention such as carbon nanotubes (CNTs) [139], graphenes [140], and metallic nanowires [141]. Among of these conductive nano-materials, 1D metallic nanowire especially silver nanowires (AgNWs) has been considered as the most potential candidate in field of transparent conductive materials since 2002 prepared by Xia's group [69]. In order to highlight the advantages of AgNWs, the first AgNWs-polymer (PET) flexible transparent electrode has been prepared by Coleman's group [70]. However, the adhesion property and thermal stability of substrate is too weak to endure higher temperature processing or long-term harsh environments. Until 2012, the requirement of thermal stability on PI/AgNWs flexible electrode was first indicated by Kim's group and applied in solar cell devices [78g]. Thus, some publications popped up for its advancing thermal stability [78,142]. Moreover, higher FoM value (180) of AgNWs-PI film was achieved in 2013 [78f]. However, the cut-off wavelength of polyimide substrate adopted in AgNWs system was still too high due to the coloration by CTC formation. The colorless AgNWs-PI hybrid electrode have been prepared and published by Liou's group [137]. However, highly transparent and flexible electrodes with the highest thermal stability were successfully prepared from PI/AgNWs hybrid solutions. The prepared highly flexible PI/AgNWs electrodes exhibited a low resistance of 25 Ω sq^1 and high transmittance up to 86% at a wavelength of 550 nm. Thus, by introducing high performance PI **P30** as a binder (Scheme 3.6), the obtained colorless PI/AgNWs electrodes showed much enhanced adhesion properties between the AgNWs and the substrate **P31** as well as thermal stability. Furthermore, the resulting PI/AgNWs hybrid colorless electrodes could maintain the conductivity even after folding more than 1000 times (Fig. 3.9). Thus, these transparent PI/AgNWs hybrid electrodes have highly potential to operate at high temperatures working environment or post processing.

4. Conclusions

The high-performance polyimides exhibit excellent thermal stability and mechanical properties. The optical transparency of PI could be improved by the introduction of bulky moieties or pendant substituents such as fluorine group. In addition, the functional PI hybrids with inorganic materials could enhance refractive index or dielectric property, and the introduction of TiO_2 served as acceptor revealed memory behavior with tunable retention time by controlling different hybrid amounts. Furthermore, the transparent and flexible conductive electrodes also could be fabricated by the combination of AgNWs and PIs. In summary, by the excellent combination of transparent PIs and inorganic materials, the resulting PI hybrids reveal interesting characteristics which are indispensable in optical and electrical applications.

Acknowledgements

The authors are grateful acknowledge to the Ministry of Science and Technology of Taiwan (104-2113-M-002 -002 -MY3) for the financial support.

References,

[1] H. Staudinger, Ber. Dtsch. Chem. Ges. 53 (1920) 1073–1085.
[2] R. Hill, E.E. Walker, J. Polym. Sci. 3 (1948) 609–630.
[3] P.E. Cassidy, Thermally Stable Polymers, Marcel Dekker, New York, 1980.
[4] (a) R.A. Dine-Hart, W.W. Wright, J. Appl. Polym. Sci. 11 (1967) 609–627;
(b) C.E. Sroog, J. Polym. Sci. Macro. Rev. 11 (1976) 161–208;
(c) V. Ratta, Faculty of Virginia Polytechnic Institute and State University(Doctoral Thesis) 1999;
(d) S. Mehdipour-Ataei, N. Bahri-Laleh, Iran. Polym. J. 17 (2008) 95–124;
(e) H.-J. Yen, G.-S. Liou, Polym. Chem. 3 (2012) 255–264.
[5] M.H. Brink, D.K. Brandom, G.L. Wilkes, J.E. McGrath, Polymer 35 (1994) 5018–5023.
[6] P.M. Cotts, Polyimides: Synthesis, Characterization and Properties, vol. 1Plenum New York, 1984.
[7] M.I. Bessonov, M.M. Koton, V.V. Kudryavtsev, L.A. Laius, Polyimides: Thermally Stable Polymers, 2 ed. Plenum, New York, 1987.
[8] (a) S.Z.D. Cheng, F.E. Arnold, A. Zhang, S.L.C. Hsu, F.W. Harris, Macromolecules 24 (1991) 5856–5862;
(b) D. Sęk, P. Pijet, A. Wanic, Polymer 33 (1992) 190–193;
(c) D. Sek, A. Wanic, E. Schab-Balcerzak, J. Polym. Sci. A Polym. Chem. 33 (1995) 547–554;
(d) S. Mehdipour-Ataei, N. Bahri-Laleh, A. Amirshaghaghi, Polym. Degrad. Stab. 91 (2006) 2622–2631.
[9] (a) R.J. Karcha, R.S. Porter, J. Polym. Sci. B Polym. Phys. 31 (1993) 821–830;
(b) X.D. Li, Z.X. Zhong, G. Jin, S.H. Lee, M.-H. Lee, Macromol. Res. 14 (2006) 257–260;
(c) S.H. Hsiao, C.H. Yu, Polym. J. 29 (1997) 944–948;
(d) H. Kawakami, K. Nakajima, H. Shimizu, S. Nagaoka, J. Membr. Sci. 212 (2003) 195–203;
(e) S.H. Hsiao, K.H. Lin, J. Polym. Sci. A Polym. Chem. 43 (2005) 331–341;
(f) M. Hasegawa, N. Sensui, Y. Shindo, R. Yokota, Macromolecules 32 (1999) 387–396;
(g) H.B. Zheng, Z.Y. Wang, Macromolecules 33 (2000) 4310–4312;
(h) P.M. Hergenrother, K.A. Watson, J.G. Smith, J.W. Connell, R. Yokota, Polymer 43 (2002) 5077–5093.
[10] (a) Y. Yang, Z.K. Zhu, J. Yin, X.Y. Wang, Z.E. Qi, Polymer 40 (1999) 4407–4414;
(b) D.J. Liaw, K.L. Wang, Y.C. Huang, K.R. Lee, J.Y. Lai, C.S. Ha, Prog. Polym. Sci. 37 (2012) 907–974;
(c) Y. Imai, React. Funct. Polym. 30 (1996) 3–15;
(d) D.J. Liaw, B.Y. Liaw, L.J. Li, B. Sillion, R. Mercier, R. Thiria, H. Sekiguchi, Chem. Mater. 10 (1998) 734–739;
(e) D. Ayala, A.E. Lozano, J. De Abajo, J.G. De La Campa, J. Polym. Sci. A Polym. Chem. 37 (1999) 805–814.
[11] (a) G. Maier, Prog. Polym. Sci. 26 (2001) 3–65;
(b) S. Ando, J. Photopolym. Sci. Technol. 17 (2004) 219–232;
(c) R. Okuda, K. Miyoshi, N. Arai, M. Tomikawa, J. Photopolym. Sci. Technol. 17 (2004) 207–213.
[12] (a) W.A. MacDonald, J. Mater. Chem. 14 (2004) 4–10;
(b) G.P. Crawford, Flexible flat panel displays, 2005;
(c) H. Ito, W. Oka, H. Goto, H. Umeda, Jpn. J. Appl. Phys. 45 (2006) 4325–4329.
[13] (a) W. Zhang, H.J. Xu, J. Yin, X.X. Guo, Y.F. Ye, J.H. Fang, J. Appl. Polym. Sci. 81 (2001) 2814–2820;
(b) H. Lim, W.J. Cho, C.S. Ha, S. Ando, Y.K. Kim, C.H. Park, Adv. Mater. 14 (2002) 1275–1279;
(c) T.L. Li, S.L.C. Hsu, Eur. Polym. J. 43 (2007) 3368–3373;
(d) M.C. Choi, L.C. Hwang, C. Kim, S. Ando, C.S. Ha, J. Polym. Sci. A Polym. Chem. 48 (2010) 1806–1814;
(e) T.L. Li, S.L.C. Hsu, Thin Solid Films 518 (2010) 6761–6766;
(f) J.M. Liu, T.M. Lee, C.H. Wen, C.M. Leu, J. Soc. Inf. Disp. 19 (2011) 63–69;
(g) K. Mizoguchi, Y. Shibasaki, M. Ueda, J. Photopolym. Sci. Technol. 20 (2007) 181–186.
[14] (a) W. Qu, T.Z. Ko, R.H. Vora, T.S. Chung, Polymer 42 (2001) 6393–6401;
(b) C. P. Yang, H. W. Yang, US Patent, 2000, 6,093,790;
(c) A.K.St. Clair, W.S. Slemp, SAMPE J. 21 (1985) 28;
(d) B.Y. Myung, J.S. Kim, T.H. Yoon, J. Polym. Sci. A Polym. Chem. 41 (2003) 3361–3374;
(e) C.P. Yang, R.S. Chen, K.H. Chen, J. Polym. Sci. A Polym. Chem. 41 (2003) 922–938;
(f) C.P. Yang, Y.Y. Su, Polymer 46 (2005) 5778–5788;
(g) S.L. Ma, Y.S. Kim, J.H. Lee, J.S. Kim, I. Kim, J.C. Won, Polymer 29 (2005) 204–210;
(h) C.P. Yang, Y.C. Chen, J. Appl. Polym. Sci. 96 (2005) 2399–2412;
(i) J.H. Kim, W.J. Koros, D.R. Paul, Polymer 47 (2006) 3094–3103;
(j) A.S. Mathews, I. Kim, C.S. Ha, Macromol. Res. 15 (2007) 114–128;
(k) K. Higashi, Y. Noda, Eur. Pat. (1986) 240249;
(l) T. Matsuura, S. Ando, S. Sasaki, F. Yamamoto, Electron. Lett. 29 (1993) 2107–2109.
[15] (a) J. Wakita, S. Ando, J. Phys. Chem. B 113 (2009) 8835–8846;
(b) Y. Sato, M. Yoshida, S. Ando, J. Photopolym. Sci. Technol. 19 (2006) 297–304;
(c) K. Takizawa, J. Wakita, S. Azami, S. Ando, Macromolecules 44 (2011) 349–359.
[16] (a) T. Hasegawa, K. Horie, Prog. Polym. Sci. 26 (2001) 259–335;
(b) C.P. Yang, Y.Y. Su, Polymer 46 (2005) 5797–5807;
(c) C.P. Yang, S.H. Hsiao, K.L. Wu, Polymer 44 (2003) 7067–7078.
[17] L. Zhai, S. Yang, L. Fan, Polymer 53 (2012) 3529–3539.
[18] M. Hasegawa, D. Hirano, M. Fujii, M. Haga, E. Takezawa, S. Yamaguchi, A. Ishikawa, T. Kagayama, J. Polym. Sci. A Polym. Chem. 51 (2013) 575–592.
[19] S. Ando, Y. Terui, Y. Aiki, T. Ishizuka, J. Photopolym. Sci. Technol. 18 (2005) 333–336.
[20] M. Hasegawa, High Perform. Polym. 13 (2001) S93–S106.
[21] S.H. Hsiao, H.M. Wang, W.J. Chen, T.M. Lee, C.M. Leu, J. Polym. Sci. A Polym. Chem. 49 (2011) 3109–3120.
[22] K.L. Mittal, Polyimides and Other High Temperature Polymers, 2003.
[23] C.P. Yang, R.S. Chen, M. Wang, J. Polym. Sci. A Polym. Chem. 40 (2002) 1092–1102.
[24] D.J. Liaw, F.C. Chang, J. Polym. Sci. A Polym. Chem. 42 (2004) 5766–5774.

Please cite this article as: C.-L. Tsai, et al., Highly transparent polyimide hybrids for optoelectronic applications, Reactive and Functional Polymers (2016), http://dx.doi.org/10.1016/j.reactfunctpolym.2016.04.021

[25] H.S. Li, J.G. Liu, K. Wang, L. Fan, S.Y. Yang, Polymer 47 (2006) 1443–1450.
[26] T. Matsuura, Y. Hasuda, S. Nishi, N. Yamada, Macromolecules 24 (1991) 5001–5005.
[27] A. K. st. Clair, T. L. st Clair, US Patent, (1986) 4,603,061.
[28] K. Han, K. You, W.H. Jang, T.H. Rhee, Macromol. Chem. Phys. 201 (2000) 747–751.
[29] (a) G.C. Eastmond, J. Paprotny, Macromolecules 28 (1995) 2140–2146;
(b) S.H. Hsiao, C.P. Yang, K.Y. Chu, Macromolecules 30 (1997) 165–170;
(c) G.C. Eastmond, J. Paprotny, R.S. Irwin, Macromolecules 29 (1996) 1382–1388.
[30] S.H. Hsiao, C.P. Yang, S.H. Chen, Polymer 41 (2000) 6537–6551.
[31] S.H. Hsiao, C.P. Yang, S.H. Chen, J. Polym. Sci. A Polym. Chem. 38 (2000) 1551–1559.
[32] T. Matsumoto, T. Kurosaki, Macromolecules 28 (1995) 5684–5685.
[33] W. Volksen, H.J. Cha, M.I. Sanchez, D.Y. Yoon, React. Funct. Polym. 30 (1996) 61–69.
[34] S. Miake, J. Kato, Y. Muroya, Y. Katsumura, T. Yamashita, J. Photopolym. Sci. Technol. 16 (2003) 255–260.
[35] T. Matsumoto, T. Kurosaki, Macromolecules 30 (1997) 993–1000.
[36] T. Ogura, M. Ueda, Macromolecules 40 (2007) 3527–3529.
[37] J. Ishii, S. Horii, N. Sensui, M. Hasegawa, L. Vladimirov, M. Kochi, R. Yokota, High Perform. Polym. 21 (2008) 282–303.
[38] J.V. Crivello, J. Polym. Sci. A Polym. Chem. 11 (1973) 1185–1200.
[39] J.E. White, D.A. Snider, J. Appl. Polym. Sci. 29 (1984) 891–899.
[40] (a) R. Hariharan, S. Bhuvana, M.A. Malbi, M. Sarojadevi, J. Appl. Polym. Sci. 93 (2004) 1846–1853;
(b) R. Hariharan, S. Bhuvana, M. Sarojadevi, High Perform. Polym. 18 (2006) 163–184;
(c) R. Hariharan, M. Sarojadevi, J. Appl. Polym. Sci. 108 (2008) 1126–1135;
(d) D.J. Liaw, B.Y. Liaw, J.J. Chen, Polymer 42 (2001) 867–872;
(e) N. Amutha, M. Sarojadevi, J. Polym. Res. 15 (2008) 487–499.
[41] C.C. Tsai, T.Y. Chao, H.L. Lin, Y.H. Liu, H.L. Chang, Y.L. Liu, R.J. Jeng, Dyes Pigments 82 (2009) 31–39.
[42] J.V. Crivello, J. Polym. Sci. A Polym. Chem. 14 (1976) 159–182.
[43] H.J. Yen, G.S. Liou, J. Mater. Chem. 20 (2010) 4080–4084.
[44] (a) C. Sanchez, B. Lebeau, F. Chaput, J.P. Boilot, Adv. Mater. 15 (2003) 1969–1994;
(b) C. Lu, B. Yang, J. Mater. Chem. 19 (2009) 2884–2901.
[45] G. Kickelbick, Hybrid Materials: Synthesis, Characterization, and Applications, Weinheim, Wiley-VCH, 2007.
[46] (a) B.M. Novak, Adv. Mater. 5 (1993) 422–433;
(b) P. Judeinstein, C. Sanchez, J. Mater. Chem. 6 (1996) 511–525;
(c) C. Sanchez, F. Ribot, New J. Chem. 18 (1994) 1007;
(d) C. Sanchez, F. Ribot, B. Lebeau, J. Mater. Chem. 35 (1999) 22.
[47] (a) T. Omote, K. Koseki, T. Yamaoka, Macromolecules 23 (1990) 4788–4795;
(b) H.S. Yu, T. Yamashita, K. Horie, Macromolecules 29 (1996) 1144–1150;
(c) M. Ueda, T. Nakayama, Macromolecules 29 (1996) 6427–6431;
(d) S. Akimoto, M. Jikei, M. Kakimoto, High Perform. Polym. 12 (2000) 177–184.
[48] (a) T.A. Chen, A.K.-Y. Jen, Y. Cai, Macromolecules 29 (1996) 535–539;
(b) E.H. Kim, I.K. Moon, H.K. Kim, M.H. Lee, S.G. Han, M.H. Yi, K.Y. Choi, Polymer 40 (1999) 6157–6167.
[49] T.A. Chen, A.K.-Y. Jen, Y. Cai, J. Am. Chem. Soc. 117 (1995) 7295–7296.
[50] T. Agag, T. Takeichi, Polymer 40 (1999) 6557–6563.
[51] (a) G.L. Tullos, L.J. Mathias, Polymer 40 (1999) 3463–3468;
(b) G.L. Tullos, J.M. Powers, S.J. Jeskey, L.J. Mathias, Macromolecules 32 (1999) 3598–3612.
[52] (a) Y.Q. Rao, S. Chen, Macromolecules 41 (2008) 4838–4844;
(b) C.J. Brinker, G.W. Scherer, Sol-Gel Science:The Physics and Chemistry of Sol-Gel Processing, first ed. Academic Press, San Diego, 1990;
(c) J.J. Ebelmen, Annals 57 (1846) 331.
[53] W. Geffcken, E. Berger, Ger. Pat. 736 (1939) 411.
[54] C.B. Hurd, Chem. Rev. 22 (1938) 403–422.
[55] M. Spinu, A.B. Brennan, K. Rancourt, G.L. Wilkes, J.E. McGrath, Mater. Res. Soc. Symp. Proc. 175 (1990) 179.
[56] (a) Y. Chen, J.O. Iroh, Chem. Mater. 11 (1999) 1218–1222;
(b) D.H. Choi, J.H. Park, T.H. Rhee, N.J. Kim, S.D. Lee, Chem. Mater. 10 (1998) 705–709.
[57] J. Brinker, G.W. Scherer, Sol-Gel Science, Academic Press, London, 1990.
[58] R. Aelion, A. Loebel, F. Eirich, J. Am. Chem. Soc. 72 (1950) 5750–5751.
[59] R.A. Assink, B.D. Kay, J. Non-Cryst. Solids 99 (1988) 359–370.
[60] (a) C.J. Brinker, K.D. Keefer, D.W. Schaefer, C.S. Ashley, J. Non-Cryst. Solids 48 (1982) 47–64;
(b) C.F. Brinker, K.D. Keefer, D.W. Schaefer, C.S. Assink, J. Non-Cryst. Solids 63 (1984) 45–59.
[61] (a) N.P. Mellott, C. Durucan, C.G. Pantano, M. Guglielmi, Thin Solid Films 502 (2006) 112–120;
(b) T. Watanabe, A. Nakajima, R. Wang, M. Minabe, S. Koizumi, A. Fujishima, K. Hashimoto, Thin Solid Films 351 (1999) 260–263;
(c) V. Roméas, P. Pichat, C. Guillard, T. Chopin, C. Lehaut, Ind. Eng. Chem. Res. 38 (1999) 3878–3885;
(d) G. Kaishu, Surf. Coat. Technol. 191 (2005) 155–160;
(e) J. Kruenate, R. Tongpool, T. Panyathanmaporn, P. Kongrat, Surf. Interface Anal. 36 (2004) 1044–1047.
[62] (a) C. Lu, Z. Cui, C. Guan, J. Guan, B. Yang, J. Sheng, Macromol. Mater. Eng. 288 (2003) 717;
(b) D. Ratna, O. Becker, R. Krishnamurthy, G.P. Simon, R.J. Varley, Polymer 44 (2003) 7449–7457;
(c) H. Mori, D.C. Seng, M. Zhang, A.H.E. Müller, Progr. Colloid Polym. Sci. 126 (2004) 40–43.
[63] (a) N.R. Choudhury, J. Sol-Gel Sci. Technol. 31 (2004) 37–45;
(b) J. Zou, Y. Zhao, W. Shi, X. Sheng, K. Nie, Polym. Adv. Technol. 16 (2005) 55–60.
[64] J. Zou, W. Shi, X. Hong, Compos. Part A 36 (2005) 631–637.
[65] L. Fogelström, P. Antoni, E. Malmström, A. Hult, Prog. Org. Coat. 55 (2006) 284–290.
[66] N. Nakayama, T. Hayashi, Compos. Part A 38 (2007) 1996–2004.
[67] L. Chen, Y. Liu, Y. Li, J. Alloys Compd. 381 (2004) 266–271.
[68] T. Otsuka, Y. Chujo, Polym. J. 42 (2010) 58–65.
[69] Y. Sun, Y. Yin, B.T. Mayers, T. Herricks, Y. Xia, Chem. Mater. 14 (2002) 4736–4745.
[70] S. De, T.M. Higgins, P.E. Lyons, E.M. Doherty, P.N. Nirmalraj, W.J. Blau, J.J. Boland, J.N. Coleman, ACS Nano 3 (2009) 1767–1774.
[71] (a) L. Hu, H.S. Kim, J.Y. Lee, P. Peumans, Y. Cui, ACS Nano 4 (2010) 2955–2963;
(b) A.R. Madaria, A. Kumar, F.N. Ishikawa, C. Zhou, Nano Res. 3 (2010) 564–573.
[72] (a) H.J. Lee, J.H. Hwang, K.B. Choi, S.G. Jung, K.N. Kim, Y.S. Shim, C.H. Park, Y.W. Park, B.K. Ju, ACS Appl. Mater. Interfaces 5 (2013) 10397–10403;
(b) P. Lee, J. Lee, H. Lee, J. Yeo, S. Hong, K.H. Nam, D. Lee, S.S. Lee, S.H. Ko, Adv. Mater. 24 (2012) 3326–3332;
(c) F. Xu, Y. Zhu, Adv. Mater. 24 (2012) 5117–5122;
(d) X. Ho, J. Nie Tey, W. Liu, C. Kweng Cheng, J. Wei, J. Appl. Phys. 113 (2013) 044311;
(e) C. Preston, Y. Xu, X. Han, J.N. Munday, L. Hu, Nano Res. 6 (2013) 461–468.
[73] (a) Z. Yu, Q. Zhang, L. Li, Q. Chen, X. Niu, J. Liu, Q. Pei, Adv. Mater. 23 (2011) 664–668;
(b) W. Hu, X. Niu, L. Li, S. Yun, Z. Yu, Q. Pei, Nanotechnology 23 (2012) 344002.
[74] (a) W. Hu, X. Niu, R. Zhao, Q. Pei, Appl. Phys. Lett. 102 (2013) 083303;
(b) H.W. Tien, S.T. Hsiao, W.H. Liao, Y.H. Yu, F.C. Lin, Y.S. Wang, S.M. Li, C.C.M. Ma, Carbon 58 (2013) 198–207;
(c) S.P. Chen, Y.C. Liao, Phys. Chem. Chem. Phys. 16 (2014) 19856–19860.
[75] (a) D. Lee, H. Lee, Y. Ahn, Y. Jeong, D.Y. Lee, Y. Lee, Nanoscale 5 (2013) 7750–7755;
(b) K. Naito, N. Yoshinaga, E. Tsutsumi, Y. Akasaka, Synth. Met. 175 (2013) 42–46.
[76] I. Moreno, N. Navascues, M. Arruebo, S. Irusta, J. Santamaria, Nanotechnology 24 (2013) 275603.
[77] (a) S. Narayanan, J.R. Hajzus, C.E. Treacy, M.R. Bockstaller, L.M. Porter, ECS J. Solid State. Sci. 3 (2014) P363–P369;
(b) J. Lee, F. Sun, J. Lee, J. Exp. Nanosci. 8 (2013) 130–137.
[78] (a) D.S. Ghosh, T.L. Chen, V. Mkhitaryan, V. Pruneri, ACS Appl. Mater. Interfaces 6 (2014) 20943–20948;
(b) C. Gong, J. Liang, W. Hu, X. Niu, S. Ma, H.T. Hahn, Q. Pei, Adv. Mater. 25 (2013) 4186–4191;
(c) T.H.L. Nguyen, L. Quiroga Cortes, A. Lonjon, E. Dantras, C. Lacabanne, J. Non-Cryst. Solids 385 (2014) 34–39;
(d) M.S. Lee, K. Lee, S.Y. Kim, H. Lee, J. Park, K.H. Choi, H.K. Kim, D.G. Kim, D.Y. Lee, S. Nam, J.U. Park, Nano Lett. 13 (2013) 2814–2821;
(e) C.Y. Lin, D.H. Kuo, W.C. Chen, M.W. Ma, G.S. Liou, Org. Electron. 13 (2012) 2469–2473;
(f) K.H. Choi, J. Kim, Y.J. Noh, S.I. Na, H.K. Kim, Sol. Energy Mater. Sol. Cells 110 (2013) 147–153;
(g) J.W. Lim, D.Y. Cho, K. Eun, S.H. Choa, S.I. Na, J. Kim, H.K. Kim, Sol. Energy Mater. Sol. Cells 105 (2012) 69–76;
(h) J. Jiu, T. Sugahara, M. Nogi, T. Araki, K. Suganuma, H. Uchida, K. Shinozaki, Nanoscale 5 (2013) 11820–11828;
(i) Q. Huang, W. Shen, X. Fang, G. Chen, J. Guo, W. Xu, R. Tan, W. Song, RSC Adv. 5 (2015) 45836–45842.
[79] (a) L.L. Beecroft, C.K. Ober, J. Macromol. Sci. Pure. Appl. Chem A 34 (1997) 573–586;
(b) J.G. Liu, M. Ueda, J. Mater. Chem. 19 (2009) 8907–8919;
(c) T. Higashihara, M. Ueda, Macromolecules 48 (2015) 1915–1929.
[80] (a) R. Morford, R. Mercado, C. Planje, T. Flaim, Proc. SPIE 5724 (2005) 34–41;
(b) T. Flaim, Y. Wang, R. Mercado, Proc. SPIE 5250 (2003) 423–434.
[81] (a) M. Ochi, Y. Maeda, K. Wakao, Jpn. J. Net. Polym. 27 (2006) 30 (in Japanese);
(b) Y.G. Ju, G. Almuneau, T.H. Kim, B.W. Lee, Jpn. J. Appl. Phys. 45 (2006) 2546–2549.
[82] K.C. Krogman, T. Druffel, M.K. Sunkara, Nanotechnology 16 (2005) S338–S343.
[83] (a) M. Suwa, H. Niwa, M. Tomikawa, J. Photopolym. Sci. Technol. 19 (2006) 275–276;
(b) J.L. Regolini, D. Benoit, P. Morin, Microelectron. Reliab. 47 (2007) 739–742.
[84] (a) F. Mammeri, E. Le Bourhis, L. Rozes, C. Sanchez, J. Mater. Chem. 15 (2005) 3787–3811;
(b) E.D. Palik, Handbook of Optical Constants of Solids, Academic Press, Orlando, 1985.
[85] (a) B.M. Novak, Adv. Mater. 5 (1993) 422;
(b) H.R. Allcock, Adv. Mater. 6 (1994) 106–115.
[86] (a) T.T. Suzuki, Macromol. Mater. Eng. 293 (2008) 109–113;
(b) M.M. Demir, M. Memesa, P. Castignolles, G. Wegner, Macromol. Rapid Commun. 27 (2006) 763–770;
(c) H. Cui, M. Zayat, P.G. Parejo, D. Levy, Adv. Mater. 20 (2008) 65–68.
[87] H. Althues, J. Henle, S. Kaskel, Chem. Soc. Rev. 36 (2007) 1454–1465.
[88] (a) K. Shinichi, T. Masashi, M. Hiroaki, F. Takeshi, K. Kana, Y. Misuaki, S. Yasuhiro, Jpn. Kokai Tokkyo JP 2005162785 (2005);
(b) R.A. Guadiana, R.A. Minns, J. Macromol. Sci. Chem. A28 (9) (1991) 831–842;
(c) R. Mercado, Y. Wang, T. Flaim, W. DiMenna, U. Senapati, Org. Photon Mater. Devices VI 5351 (2004) 276–283.
[89] J.G. Liu, Y. Nakamura, Y. Shibasaki, S. Ando, M. Ueda, J. Polym. Sci. A Polym. Chem. 45 (2007) 5606–5617.
[90] (a) C. Paquet, P.W. Cyr, E. Kumacheva, I. Manners, Chem. Mater. 16 (2004) 5205–5211;
(b) A.D. Pomogailo, Russ. Chem. Rev. 69 (2000) 53–80.
[91] T. Matsuda, Y. Funae, M. Yoshida, T. Tsuguo, J. Macromol. Sci. Pure Appl. Chem. A36 (1999) 1271–1288.
[92] R.A. Minns, R.A. Gaudiana, J. Macromol. Sci. Pure Appl. Chem. A29 (1992) 19–30.

Please cite this article as: C.-L. Tsai, et al., Highly transparent polyimide hybrids for optoelectronic applications, Reactive and Functional Polymers (2016), http://dx.doi.org/10.1016/j.reactfunctpolym.2016.04.021

[93] T. Matsuda, Y. Funae, M. Yoshida, T. Yamamoto, T. Takaya, J. Appl. Polym. Sci. 76 (2000) 45–49.
[94] C.L. Lu, Z.C. Cui, Y.X. Wang, B. Yang, J.C. Shen, J. Appl. Polym. Sci. 89 (2003) 2426–2430.
[95] A. Nebioglu, J. Leon, I.V.A. Khudyakov, Ind. Eng. Chem. Res. 47 (2008) 2155–2159.
[96] J.G. Liu, Y. Shibasaki, S. Ando, M. Ueda, High Perform. Polym. 20 (2008) 221–237.
[97] (a) J.G. Liu, Y. Nakamura, C.A. Terraza, Y. Suzuki, Y. Shibasaki, S. Ando, Macromol. Chem. Phys. 209 (2008) 195–203;
(b) J.G. Liu, Y. Nakamura, Y. Shibasaki, S. Ando, M. Ueda, Polym. J. 39 (2007) 543–550;
(c) J.G. Liu, Y. Nakamura, Y. Suzuki, Y. Shibasaki, S. Ando, M. Ueda, Macromolecules 40 (2007) 7902–7909;
(d) C.A. Terraza, J.G. Liu, Y. Nakamura, Y. Shibasaki, S. Ando, M. Ueda, J. Polym. Sci. A Polym. Chem. 46 (2008) 1510–1520.
[98] (a) C.C. Chang, W.C. Chen, J. Polym. Sci. Polym. Chem. 39 (2001) 3419–3427;
(b) C.M. Chang, C.L. Chang, C.C. Chang, Macromol. Mater. Eng. 291 (2006) 1521–1528;
(c) P.C. Chiang, W.T. Whang, Polymer 44 (2003) 2249–2254.
[99] J.G. Liu, Y. Nakamura, T. Ogura, Y. Shibasaki, S. Ando, M. Ueda, Chem. Mater. 20 (2008) 273–281.
[100] H.W. Su, W.C. Chen, J. Mater. Chem. 18 (2008) 1139–1145.
[101] (a) G.S. Liou, P.H. Lin, H.J. Yen, Y.Y. Yu, T.W. Tsai, W.C. Chen, J. Mater. Chem. 20 (2010) 531–536;
(b) C.L. Tsai, H.J. Yen, W.C. Chen, G.S. Liou, J. Mater. Chem. 22 (2012) 17236–17244;
(c) H.J. Yen, C.L. Tsai, P.H. Wang, G.S. Liou, RSC Adv. 3 (2013) 17048–17056.
[102] (a) P. Xue, J. Wang, Y. Bao, Q. Li, C. Wuac, New J. Chem. 36 (2012) 903–910;
(b) S.C. Yang, S.Y. Kwak, J.H. Jin, J.S. Kim, Y. Choi, K.W. Paikb, B.S. Bae, J. Mater. Chem. 22 (2012) 8874–8880;
(c) P. Gomez-Romero, C. Sanchez (Eds.), Functional Hybrid Materials, Wiley-VCH, Weinheim, 2004;
(d) G. Kickelbick, Hybrid Materials: Synthesis, Characterization, and Applications, Wiley-VCH, Weinheim, 2007.
[103] C.L. Tsai, G.S. Liou, Chem. Commun. 51 (2015) 13523–13526.
[104] (a) M. Zelner, H. Minti, R. Reisfeld, H. Cohen, R. Tenne, Chem. Mater. 9 (1997) 2541–2543;
(b) A. Sashchiuk, E. Lifshitz, R. Reisfeld, T. Saraidarov, M. Zelner, A. Willenz, J. Sol-Gel Sci. Technol. 24 (2002) 31–38;
(c) M.T. Wang, T.H. Wang, J. Lee, Microelectron. Reliab. 45 (2005) 969–972.
[105] A. Thelen, Design of Optical Interference Coatings, McGraw-Hill, New York, 1989.
[106] Q.D. Ling, D.J. Liaw, C. Zhu, D.S.H. Chan, E.T. Kang, K.G. Neoh, Prog. Polym. Sci. 33 (2008) 917–978.
[107] T. Kurosawa, T. Higashihara, M. Ueda, Polym. Chem. 3 (2013) 16–30.
[108] S.H. Cheng, S.H. Hsiao, T.H. Su, G.S. Liou, Macromolecules 38 (2005) 307–316.
[109] Q.D. Ling, F.C. Chang, Y. Song, C.X. Zhu, D.J. Liaw, D.S.H. Chan, E.T. Kang, K.G. Neoh, J. Am. Chem. Soc. 128 (2006) 8732–8733.
[110] Y.L. Liu, Q.D. Ling, E.T. Kang, K.G. Neoh, D.J. Liaw, K.L. Wang, W.T. Liou, C.X. Zhu, D.S.H. Chan, J. Appl. Phys. 105 (2009) 044501.
[111] Y.L. Liu, K.L. Wang, G.S. Huang, C.X. Zhu, E.S. Tok, K.G. Neoh, E.T. Kang, Chem. Mater. 21 (2009) 3391–3399.
[112] T.J. Lee, C.W. Chang, S.G. Hahm, K. Kim, S. Park, D.M. Kim, J. Kim, W.S. Kwon, G.S. Liou, M. Ree, Nanotechnology 20 (2009) 135204.
[113] K. Kim, S. Park, S.G. Hahm, T.J. Lee, D.M. Kim, W. Kwon, Y.G. Ko, M. Ree, J. Phys. Chem. B 113 (2009) 9143–9150.
[114] D.M. Kim, S. Park, T.J. Lee, S.G. Hahm, K. Kim, J.C. Kim, W. Kwon, M. Ree, Langmuir 25 (2009) 11713–11719.
[115] (a) N.H. You, C.C. Chueh, C.L. Liu, M. Ueda, W.C. Chen, Macromolecules 42 (2009) 4456–4463;
(b) T. Kuorosawa, C.C. Chueh, C.L. Liu, T. Higashihara, M. Ueda, W.C. Chen, Macromolecules 43 (2010) 1236–1244.
[116] (a) J. Ouyang, C.W. Chu, C.R. Szmanda, L. Ma, Y. Yang, Nat. Mater. 3 (2004) 918–922;
(b) C.W. Chu, J. Ouyang, J.H. Tseng, Y. Yang, Adv. Mater. 17 (2005) 1440–1443.
[117] (a) F. Li, T.W. Kim, W. Dong, Y.H. Kim, Appl. Phys. Lett. 92 (2008) 011906;
(b) F. Li, D.I. Son, S.M. Seo, H.M. Cha, H.J. Kim, B.J. Kim, J.H. Jung, T.W. Kim, Appl. Phys. Lett. 91 (2007) 122111.
[118] C.J. Chen, Y.C. Hu, G.S. Liou, Chem. Commun. 49 (2013) 2804–2806.
[119] C.J. Chen, J.H. Wu, G.S. Liou, Chem. Commun. 50 (2014) 4335–4337.
[120] (a) C.L. Tsai, C.J. Chen, P.H. Wang, J.J. Lin, G.S. Liou, Polym. Chem. 4 (2013) 4570–4573;
(b) C.J. Chen, C.L. Tsai, G.S. Liou, J. Mater. Chem. C 2 (2014) 2842–2850.
[121] J.S. Li, Y.J. Lin, H.P. Lu, L. Wang, S.P. Rwei, Thin Solid Films 511 (2006) 182–186.
[122] (a) A.D. Yu, C.L. Liu, W.C. Chen, Chem. Commun. 48 (2012) 383–385;
(b) S.L. Lian, C.L. Liu, W.C. Chen, Appl. Mater. Interfaces 3 (2011) 4504–4511;
(c) L. Li, Q.D. Ling, C. Zhu, D.S.H. Chan, E.T. Kang, K.G. Neoh, J. Electrochem. Soc. 155 (2008) H205–H209;
(d) Q. Zhang, J. Pan, X. Yi, L. Li, S. Shang, Org. Electron. 13 (2012) 1289–1486;
(e) J.C. Hsu, C.L. Liu, W.C. Chen, K. Sugiyama, A. Hirao, Macromol. Rapid Commun. 32 (2011) 528–533.
[123] B. Cho, T.W. Kim, M. Choe, G. Wang, S. Song, T. Lee, Org. Electron. 10 (2009) 473–477.
[124] (a) K.K. Ghuman, C.V. Singh, J. Phys. Condens. Matter 25 (2013) 475501;
(b) M. Rahman, D. MacElroy, D.P. Dowling, J. Nanosci. Nanotechnol. 11 (2011) 8642–8651;
(c) B. Ohtani, Y. Ogawa, S.I. Nishimoto, J. Phys. Chem. B 101 (1997) 3746–3752.
[125] Y. Guo, C.-a. Di, S. Ye, X. Sun, J. Zheng, Y. Wen, W. Wu, G. Yu, Y. Liu, Adv. Mater. 21 (2009) 1954–1959.
[126] (a) H.E. Katz, X.M. Hong, A. Dodabalapur, R. Sarpeshkar, J. Appl. Phys. 91 (2002) 1572–1576;
(b) K.J. Baeg, Y.Y. Noh, J. Ghim, S.J. Kang, H. Lee, D.Y. Kim, Adv. Mater. 18 (2006) 3179–3183.
[127] (a) R. Schroeder, L.A. Majewski, M. Grell, Adv. Mater. 16 (2004) 633–636;
(b) S.H. Lim, A.C. Rastogi, S.B. Desu, J. Appl. Phys. 96 (2004) 5673–5682.
[128] (a) W.L. Leong, N. Mathews, S. Mhaisalkar, Y.M. Lam, T. Chen, P.S. Lee, J. Mater. Chem. 19 (2009) 7354–7361;
(b) K.J. Baeg, Y.Y. Noh, H. Sirringhaus, D.Y. Kim, Adv. Funct. Mater. 20 (2010) 224–230;
(c) M. Burkhardt, A. Jedaa, M. Novak, A. Ebel, K. Voïtchovsky, F. Stellacci, A. Hirsch, M. Halik, Adv. Mater. 22 (2010) 2525–2528.
[129] K.J. Baeg, Y.Y. Noh, J. Ghim, B. Lim, D.Y. Kim, Adv. Funct. Mater. 18 (2008) 3678–3685.
[130] Y.H. Chou, S. Takasugi, R. Goseki, T. Ishizone, W.C. Chen, Polym. Chem. 5 (2014) 1063–1071.
[131] Y.H. Chou, N.H. You, T. Kurosawa, W.Y. Lee, T. Higashihara, M. Ueda, W.C. Chen, Macromolecules 45 (2012) 6946–6956.
[132] Y.H. Chou, H.J. Yen, C.L. Tsai, W.Y. Lee, G.S. Liou, W.C. Chen, J. Mater. Chem. C 1 (2013) 3235–3243.
[133] W.H. Lee, C.C. Wang, W.T. Chen, J.C. Ho, Jpn. J. Appl. Phys. 47 (2008) 8955–8960.
[134] Y.H. Chou, C.L. Tsai, W.C. Chen, G.S. Liou, Polym. Chem. 5 (2014) 6718–6727.
[135] (a) X. Zhang, X. Yan, J. Chen, J. Zhao, Carbon 69 (2014) 437–443;
(b) J. Li, J. Liang, X. Jian, W. Hu, J. Li, Q. Pei, Macromol. Mater. Eng. 299 (2014) 1403–1409.
[136] (a) S. Sorel, D. Bellet, J.N. Coleman, ACS Nano 8 (2014) 4805–4814;
(b) S. Ji, W. He, K. Wang, Y. Ran, C. Ye, Small 10 (2014) 4951–4960.
[137] H.Y. Lu, C.Y. Chou, J.H. Wu, J.J. Lin, G.S. Liou, J. Mater. Chem. C 3 (2015) 3629–3635.
[138] K. Alzoubi, M.M. Hamasha, S. Lu, B. Sammakia, J. Disp. Technol. 7 (2011) 593–600.
[139] S. Iijima, Nature 354 (1991) 56–58.
[140] K.S. Novoselov, A.K. Geim, S.V. Morozov, D. Jiang, Y. Zhang, S.V. Dubonos, I.V. Grigorieva, A.A. Firsov, Science 306 (2004) 666–669.
[141] (a) J.Y. Lee, S.T. Connor, Y. Cui, P. Peumans, Nano Lett. 8 (2008) 689–692;
(b) A.R. Rathmell, B.J. Wiley, Adv. Mater. 23 (2011) 4798–4803.
[142] X. Guo, X. Liu, J. Luo, Z. Gan, Z. Meng, N. Zhang, RSC Adv. 5 (2015) 24953–24959.

Please cite this article as: C.-L. Tsai, et al., Highly transparent polyimide hybrids for optoelectronic applications, Reactive and Functional Polymers (2016), http://dx.doi.org/10.1016/j.reactfunctpolym.2016.04.021